

CHAPTER D-7 FOUNDATION RISKS FOR CONCRETE DAMS

D-7.1 Key Concepts

Most historical failures of concrete dams can be traced to deficiencies in their foundations. Therefore, it is extremely important to understand the geologic conditions and geomechanical properties associated with the foundations of concrete dams to the extent possible. This requires collecting, interpreting, and portraying the geologic data in a manner that can be communicated, understood, and evaluated within the context of a potential failure mode (see chapter in this manual on geologic information needed for a risk analysis).

Backward erosion piping or internal erosion is the leading cause of failure of concrete dams that are founded on soil or river alluvium. This failure case is not covered in detail in this chapter. However, the concepts and procedures described in the chapter on internal erosion in this manual can be used to assess this type of potential failure mode. Appendix F of Scott (1999) can be used to evaluate the piping potential of filled fault and shear zones.

For concrete dams founded on rock, sliding on discontinuities (e.g. joints, fracture zones, intrusion contacts, faults, shears, bedding, foliation, etc...) within the foundation rock mass is the leading cause of historical failures. Therefore, in addition to the rock units, it is important to understand the type, location, orientation, distribution, continuity, spacing, and characteristics of the discontinuities within the foundation rock mass. All relevant information should be portrayed on geologic plan maps, cross sections, structural contour maps, and stereographic projections so that the risk analysis team can visualize the three-dimensional geometry of the foundation discontinuities. Potentially unstable foundation wedges, that have the potential to displace under the applied loads applied by the wedge weight, the dam, the reservoir, uplift pressures, and any dynamic seismic response causing rupture of the dam, can then be identified by the team and evaluated within a risk context. Assessing the stability and ultimately risks associated with potentially unstable foundation wedges requires some knowledge not only about the geometry, and location of the wedge, but also about the external loading from the dam, the water forces acting normal to the wedge planes, the shear strength of the planes forming the



wedge, and inertia forces caused by earthquake shaking (where appropriate). This information can be used to conduct a kinematic analysis to determine the mode and direction of potential sliding. This chapter is not an all-inclusive discussion of how to perform a concrete dam foundation assessment, but an attempt is made to summarize some of the key points that should be considered when performing such an evaluation. In this chapter, the dam “abutments” are considered to be part of the “foundation”.

D-7.2 Foundation Sliding Stability

Perhaps the most critical area for evaluating the foundation of a concrete dam has to do with sliding along geologic discontinuities within the abutment or foundation of a dam. Planes or intersections of planes that daylight downstream and form wedges upon which the dam rests should be identified and evaluated for sliding stability. Figure D-7-1 shows schematically how such a wedge might form, and the forces acting on such a wedge. In this case it is likely the wedge would tend to slide along the intersection of Plane 1 and Plane 2 under the applied loads.

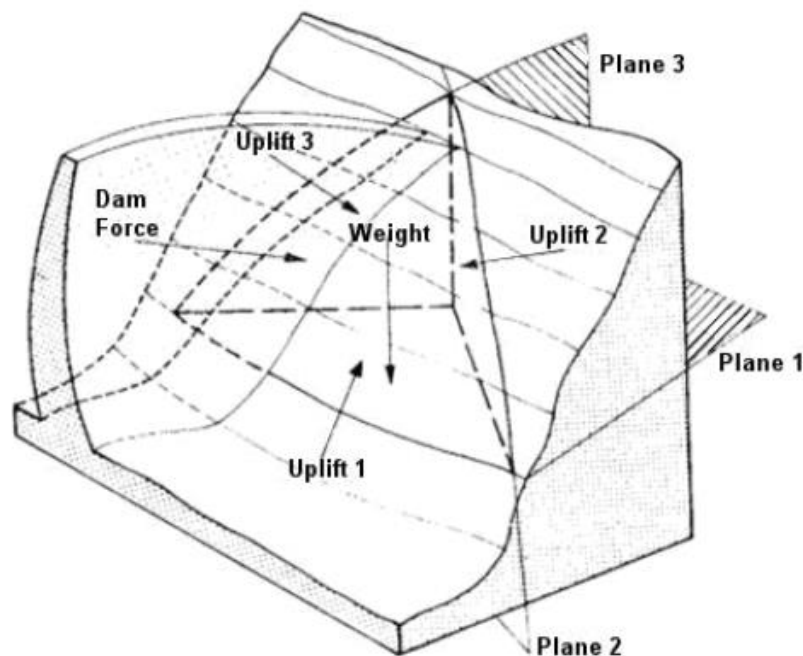


Figure D-7-1 Example of Potentially Unstable Foundation Wedge (adapted from Londe, 1973)

One step in identifying potentially unstable foundation wedges requires carefully searching available foundation maps, construction photographs, drill hole data, LiDAR analysis, and/or lineation mapping for characterizing discontinuities important to stability, particularly continuous low angle base planes that may daylight (i.e. intersect with the downstream topography in a manner that allows movement) downstream along with continuous side planes. The search should continue downstream of the foundation contact where discontinuities may be visible or were mapped. In the past, it was common to map the foundation in detail; however the areas downstream of the abutments were not always exposed and were often unmapped. This is a very important area to investigate, looking for daylighting discontinuities that could influence stability. Critical low angle planes may not be visible in the foundation. Construction photographs can be invaluable in identifying discontinuities in this area, as well as in the excavation footprint, as shown in Figure D-7-2.

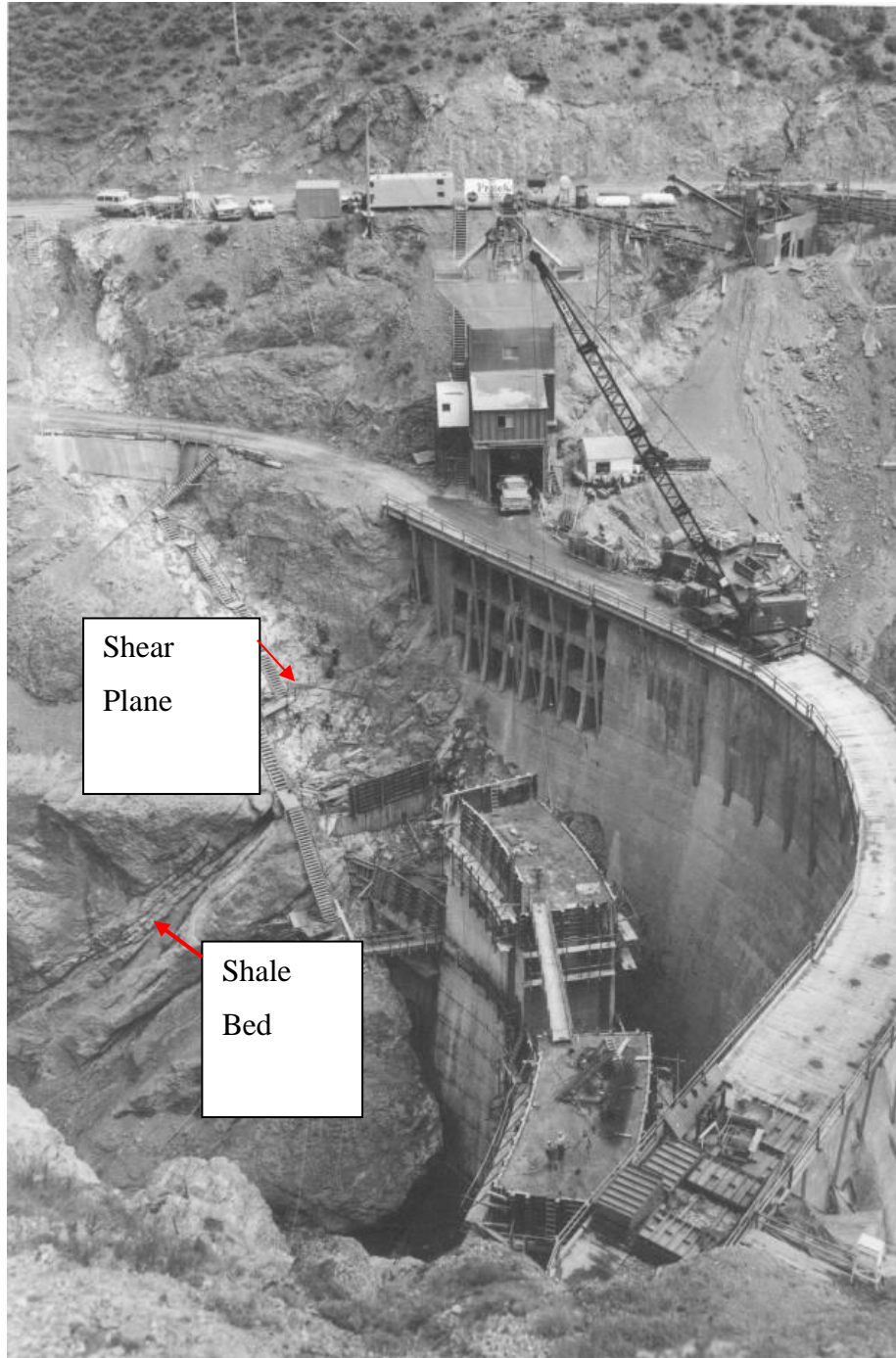


Figure D-7-2 Construction Photo Showing Major Discontinuities (note new arch dam being constructed immediately downstream of an existing arch dam)

Major discontinuities that are continuous relative to the foundation dimensions and potentially weak in shear (or that can release in tension near the upstream wedge boundary) should be identified, and their location, orientation, and characteristics should be defined. It is important to portray the geologic information on plan maps, cross sections, profiles, and structural contour maps so that the geometry is well understood and appropriate evaluations and calculations can be made. Figure D-7-3 shows example structural contours on prominent clay-coated bedding plane partings and faults. For this project, a difference in several degrees of bedding strike had a large influence on calculated stability. Information from many different sources was combined to develop structural contours for each fault and prominent “EP (Engineering Plane) bedding plane”. These planes represented potential sliding surfaces that included multiple bedding planes that aligned across faults. Data available included: preconstruction exploration; construction mapping of the foundation and adits; construction photographs of the foundation; and post construction drilling and borehole geophysics performed in the existing drain holes. EP3 was identified as the critical potential slide plane based on its close proximity to the dam foundation contact, and its extent from fault 1 at the upstream end of the dam down to fault 4 towards the bottom of the abutment. EP3 daylights downstream along with its intersections with several faults on the abutment.

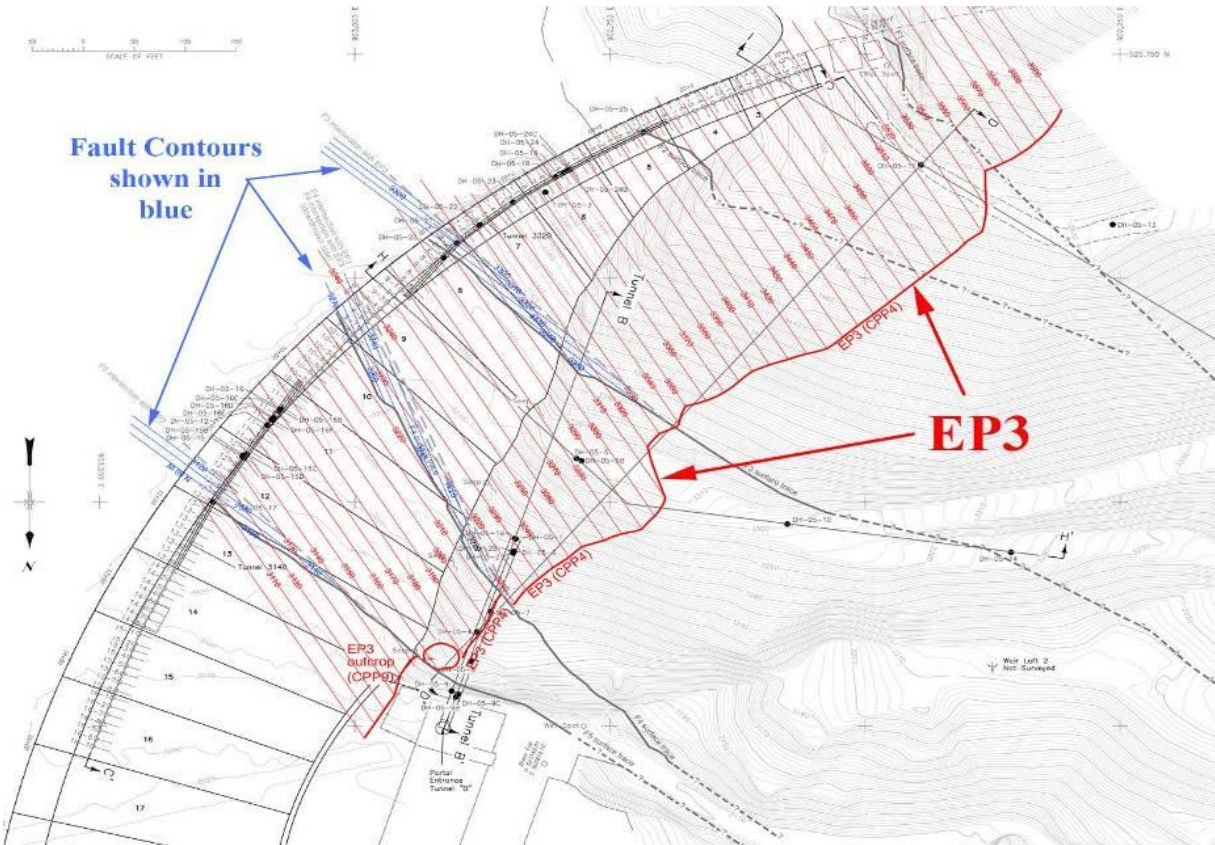


Figure D-7-3 Structural Contours on Major Discontinuities

Although the major discontinuity features are of most concern, joint patterns within the rock mass must also be considered. The orientation, continuity, spacing, alteration, infilling, weathering, roughness, small to large-scale undulations or waviness, and other characteristics need to be determined. Although typically not as continuous as the major discontinuities, secondary features can form wedge boundaries, perhaps in a stepped fashion. Intersecting joints can form a back release surface that is typically loaded in tension for a foundation wedge. Joint orientations are generally defined by dip and dip direction or strike and dip. Joint sets can be defined by contouring poles (lines normal to the joint planes) on a stereonet, to define the central tendencies and the variation in their orientations.

If no wedges can be identified that could potentially displace and cause damage to the dam under the applied loads, and an adequate and well composed case can be built, then perhaps this potential failure mode can be considered to pose negligible risk without additional analysis. However, once a potentially unstable foundation wedge has been identified, and it appears that it could possibly move and rupture the dam under the applied loads, further evaluations are needed to evaluate its stability. This may require some additional knowledge the wedge weight (and inertia forces for dynamic analyses), the water pressures acting normal to the wedge planes that reduce the effective normal stress, the shear strength of the planes forming the wedge, and the loading from the dam. These are discussed in the following sections.

D-7.3 Discontinuity Shear Strength

The shear strength of discontinuities forming foundation wedges can be critical to stability. If it can be shown, using statistics and sound arguments relative to location, that the joint set(s) forming a wedge are discontinuous such that there is significant strong intact rock that must be broken for the wedge to move, then perhaps the potential failure mode can be considered to pose negligible risk at that stage. If not, additional analysis is probably warranted, and the shear strength of potential sliding planes must be estimated. Because cohesion is so difficult to estimate and has such a profound effect on the stability analysis results, only effective stress frictional resistance is typically assumed for continuous rock discontinuities. The rough nature of natural fractures and discontinuities adds to this strength and can be taken into account. There are several methods for estimating discontinuity shear strength. They will not all be presented here (refer to Scott, 1999 for additional information). Regardless of the method used, scale effects must be considered.

Bandis et al (1983) performed direct shear tests on samples of natural fractures as shown in Figure D-7-4. They started by testing a large specimen, then proceeded to cut it into smaller and smaller specimens. On average, the strengths increased as the specimens became smaller. This indicates that the small scale asperities are not mobilized when shearing large scale joints, and testing of small scale rough joint specimens can therefore overpredict the strength. Some have proposed testing saw cuts to overcome this issue and estimate a basic friction angle for a given rock type. However, this leads to more uncertainty as most saw blades can polish the surface

smoother than the individual rock grains leading to conservative estimates of the basic friction angle. Attempts to artificially roughen a saw cut surface can result in significant variation and uncertainty as well, and any alteration along the joint surfaces is not taken into account with such an approach. A better approach to determining the basic friction angle seems to include subtracting the specimen dilation by measuring the normal and shear displacement during testing. The slope of the normal displacement vs. shear displacement curve at the point of sliding is the dilatency angle. Figure D-7-5 shows the relevant plots from a direct shear test.

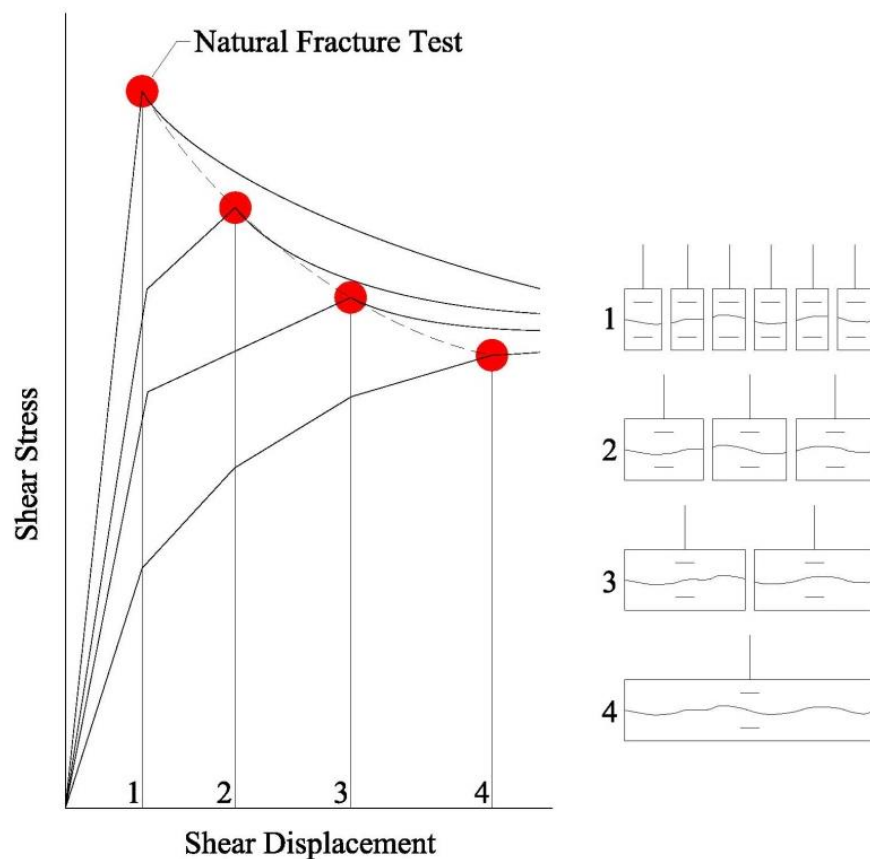


Figure D-7-4 Scale Effects from Testing Natural Joints (adapted from Bandis et al, 1983)

Once the dilatency slope, i , is determined, the strength can be corrected by solving the following equation iteratively for $\sigma \tan \phi$, where ϕ is the basic friction angle:

$$\tau_{\phi+i} = \frac{\tan \phi + \tan i}{1 - \tan \phi * \tan i} * \sigma \quad \text{Equation D-7-1}$$

The scatter in the corrected data should be reduced over that obtained from the raw test data. Once a basic friction angle has been established, the large scale asperity angles or undulations can be added to obtain an estimate of effective in situ friction angle. This typically requires some field measurements. Photogrammetry models (see chapter on geological information needed for a risk analysis) of large discontinuity surfaces can be useful for making these measurements. Typically, angles are measured along a large scale discontinuity profile using increasing step width (constructed as consecutive segments along the profile). The asperity angles are plotted as a function of step width as shown in Figure D-7-6. The asperity angle may converge to a steady state value, or a value that corresponds to 1 to 2 percent of the in situ sliding plane length has sometimes been selected to represent the waviness angle to be added to the basic friction angle. For probabilistic analyses, ranges or distributions in both the basic friction angle and waviness angle should be considered.

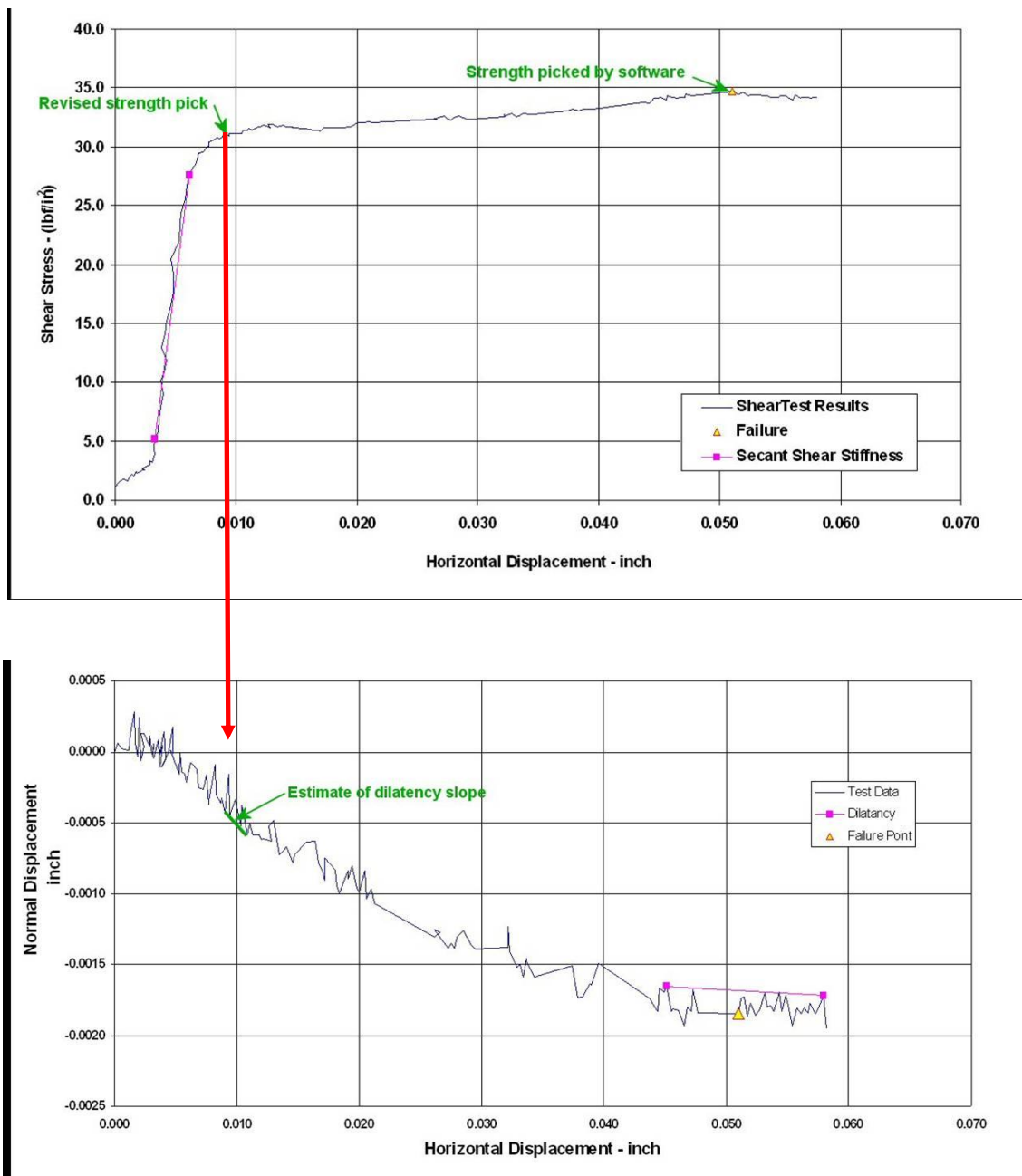


Figure D-7-5 Direct Shear Test Plots

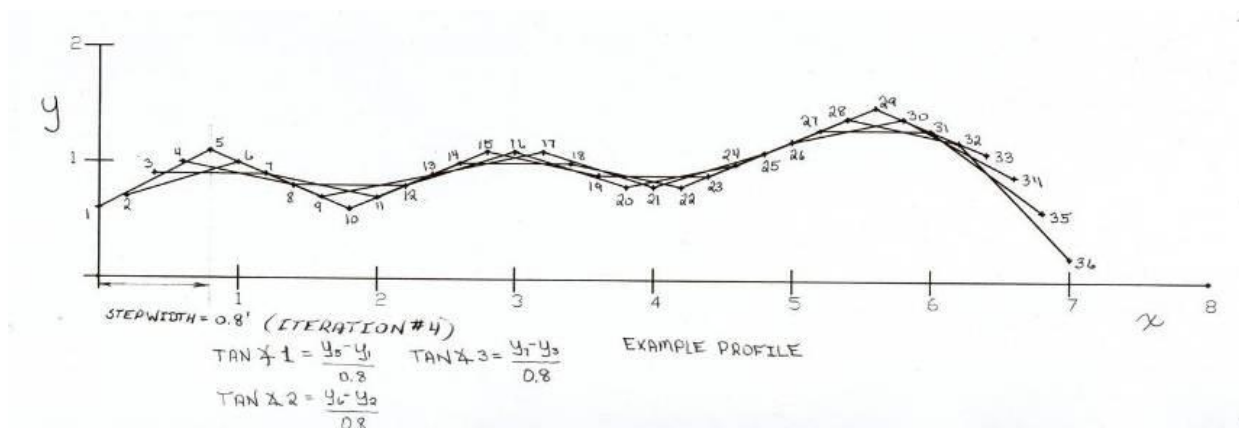
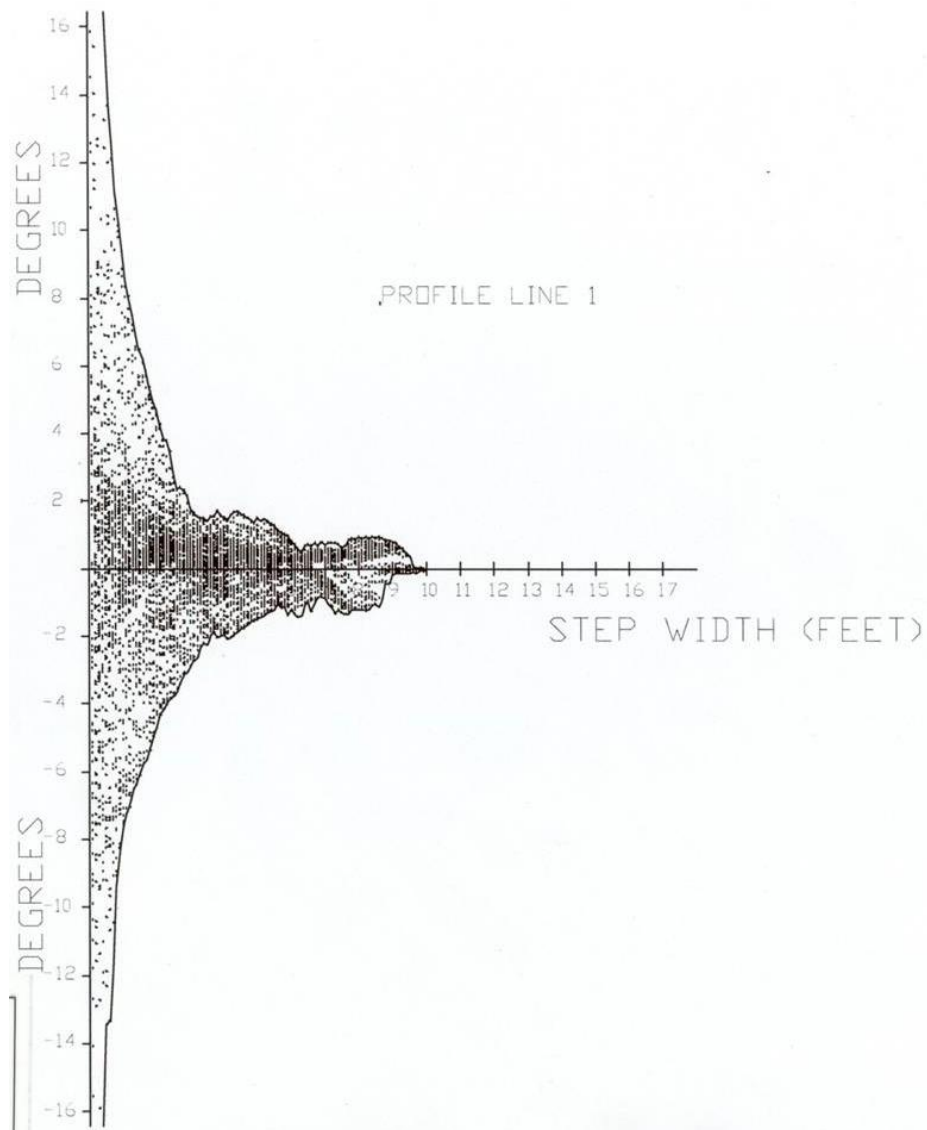


Figure D-7-6 Waviness Angle Analysis (after Rengers, 1970)

In some cases a critical sliding plane will be filled with softer infilling material, and the strength of the filling material will have a major effect on its shear strength. It can also affect the roughness or waviness component of the shear strength as the filling material compresses during shearing. To account for this, Ladanyi and Archambault (1977) have proposed some relationships that are plotted in Figure D-7-7. An effective roughness angle can be estimated based on the ratio of the Filling Thickness/Rock Wall Amplitude. Again, ranges or distributions should be considered when performing probabilistic analyses.

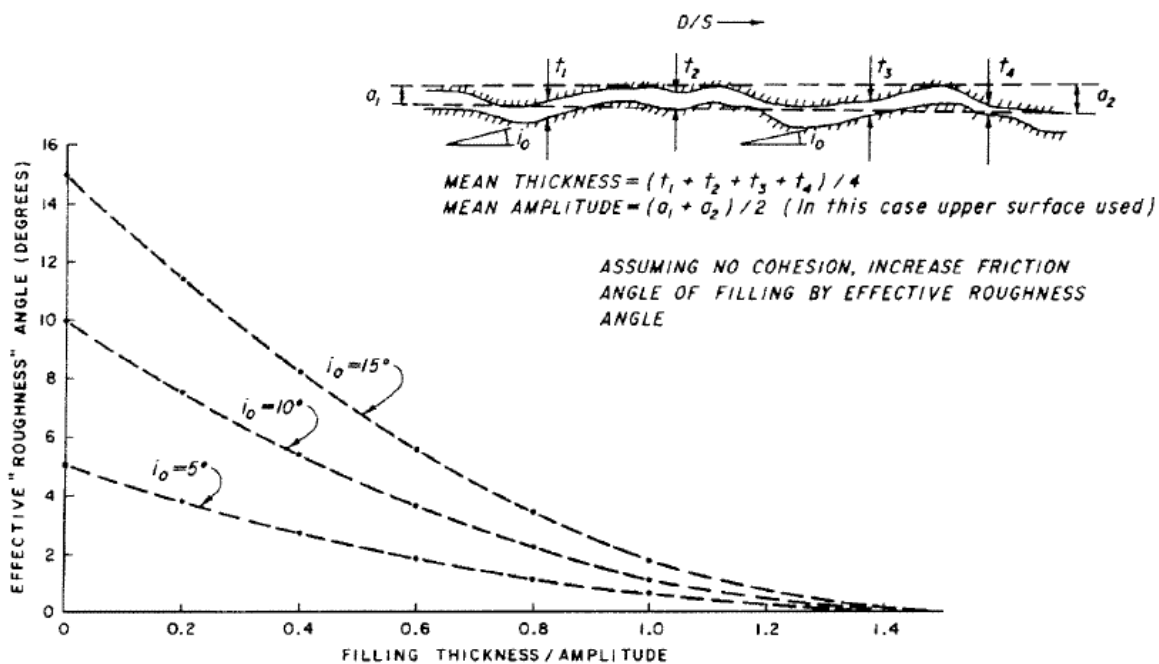


Figure D-7-7 Effective Waviness Angle for Filled Discontinuities (adapted from Ladanyi and Archambault, 1977)

D-7.4 Foundation Water Pressures

Water pressures acting normal to planes forming potentially unstable foundation wedges reduce the effective normal stress acting across those planes and therefore reduce the frictional strength that is mobilized. Estimating water pressures within the foundation of a concrete dam may therefore be critical to determining its stability.

Despite the advancements in seepage modeling that are available, experience suggests that it is difficult to model flow through jointed rock and accurately predict foundation water pressures. Therefore, typically foundation pressures are measured at key points using piezometers installed in areas of water conduits. If enough piezometers are installed, water pressure contour maps can be generated as shown in Figure D-7-8.

Care must be taken to assure the pressures portrayed are within a uniform flow or seepage zone. Separate diagrams may be needed for confined aquifers, etc. Although such diagrams assume the equipotential lines are essentially vertical, they are often more representative than results from a seepage model. Pressures can be extrapolated to reservoir and tailwater levels different from those present when the piezometric pressures were measured using the differential head ratio (DHR). The DHR, equal to $(\text{Piezometric El} - \text{Tailwater El}) / (\text{Reservoir El} - \text{Tailwater El})$, is calculated for a given set of measurements. Then the piezometric elevation can be calculated using the DHR, new reservoir level, and new tailwater level. This may underestimate the pressures close to the upstream heel of the dam where moments from higher reservoir loading can create tensile zones and higher water pressures. However, this is usually fairly localized. In addition, seismic shaking can open joints which can increase water pressures.

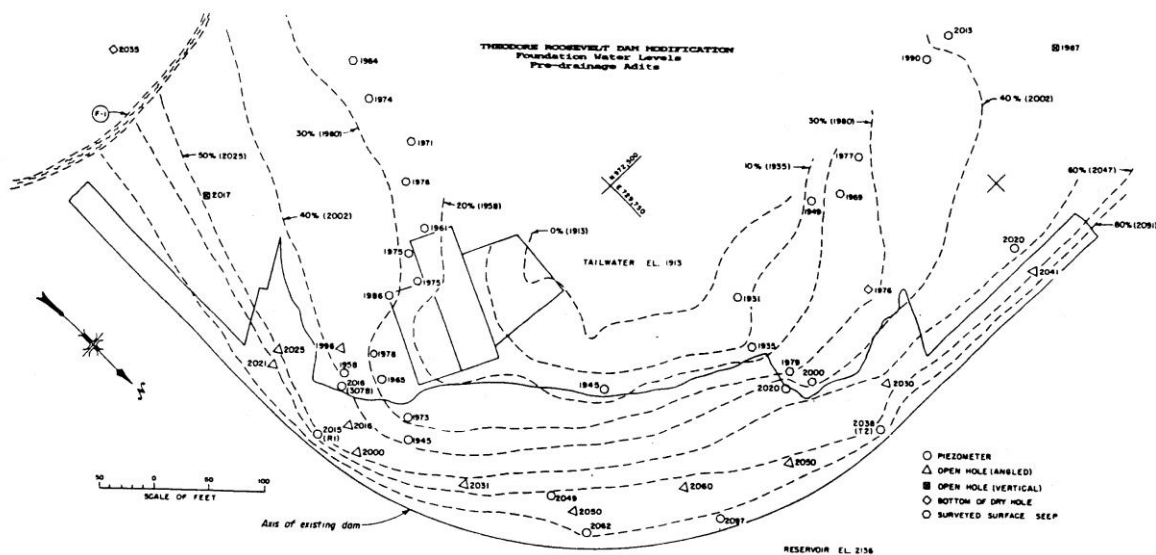


Figure D-7-8 Foundation Water Pressure Contour Map

The water pressure contour map, and structural contour map of the foundation wedge planes can be used to estimate water pressures and total water force acting normal to the planes. Sufficient piezometer data may not be available, in which case interpretations of the groundwater contours and elevations may need to be predicted or inferred based on modeling or rules-of-thumb. The intersection of the phreatic surface with the wedge planes must be determined unless the wedge planes are fully submerged. Then, using the water pressure contours, the plane is divided into areas across which the variation in water pressure is generally uniform. The pressures at each corner of these areas are calculated by subtracting the elevation of the point on the plane from the elevation of the water pressure contour directly above it. The average pressure multiplied by the area gives a force, and the summation of all such forces gives a total force on the plane.

A line of drains is typically installed as a defensive measure in a concrete dam foundation. If functioning, the drains can dramatically reduce the foundation water pressures, which would be reflected in the water pressure contours. Measurements just below the foundation contact of several large concrete dams show that the pressures downstream of a line of functioning drains are greatly reduced by the drainage, as shown in Figure D-7-9. It can be noted that the original measurements made at Hoover Dam and Owyhee Dam did not show as much pressure reduction.

However, additional deeper drains were drilled and the pressures were brought down. In that regard, it is necessary that the drains penetrate the major zone of seepage. Typically drains at about 40 percent of the hydraulic height into the foundation are adequate for this purpose. Shallower drains can also be effective if the major zone of seepage is more shallow, but it may be necessary to measure foundation pressures at depth to verify this. It is important to clean and maintain the drains in operating conditions for an adequate defensive measure.

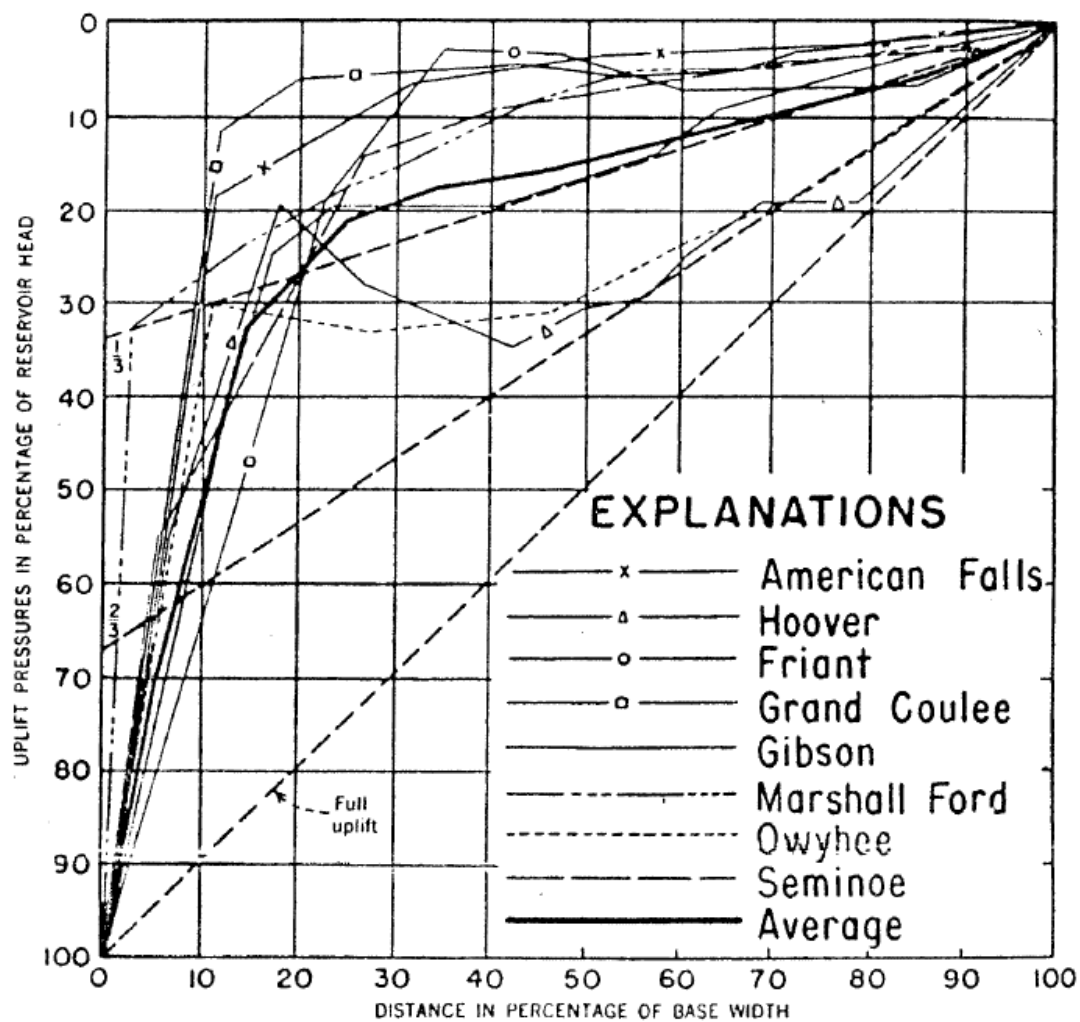


Figure D-7-9 Uplift Measurements at Concrete Dams

So what about grouting? It is often claimed that a grout curtain reduces the foundation water pressures. There have been a few cases where measurements seem to verify this. However, in the 1st Rankine Lecture, Arthur Casagrande showed that for a fully penetrating cutoff, the cutoff efficiency drops to very low values with even a small percentage of open space in the cutoff. He also pointed to measurements made within the foundation of an embankment dam where there was very little pressure drop across the grout curtain. If we think about it, although the grout holes are drilled in a line, the injected grout will travel in the direction of least resistance which could be in all directions. Therefore, a wide zone is typically grouted and not a narrow “curtain”, and therefore one would not expect a sharp drop across the line of grout holes. If the grout curtain is being counted on to reduce foundation water pressures, it is essential that measurements be made to verify this is the case.

A special caution is needed when grouting under reservoir head. Experience at several dams has shown that the grout tends to travel downstream under the flowing water, and sets up in a downstream location. This can then form a reduced permeability zone downstream which backs pressures up toward the upstream area under the dam, which can actually create a worse situation from a foundation water pressure standpoint.

D-7.5 Dam Loading and Foundation Rock Mass Modulus

Loading from the dam is needed to complete a foundation stability analysis. Initially, uncoupled analyses are typically performed whereby external loading from the dam is calculated and applied to the foundation wedge in a rigid wedge limit equilibrium analysis. Finite element analyses are often used for such calculations, whereby the nodal forces from elements contacting the wedge, as shown in Figure D-7-10, are used to estimate the external loading. Forces can be time-varying for seismic analyses.

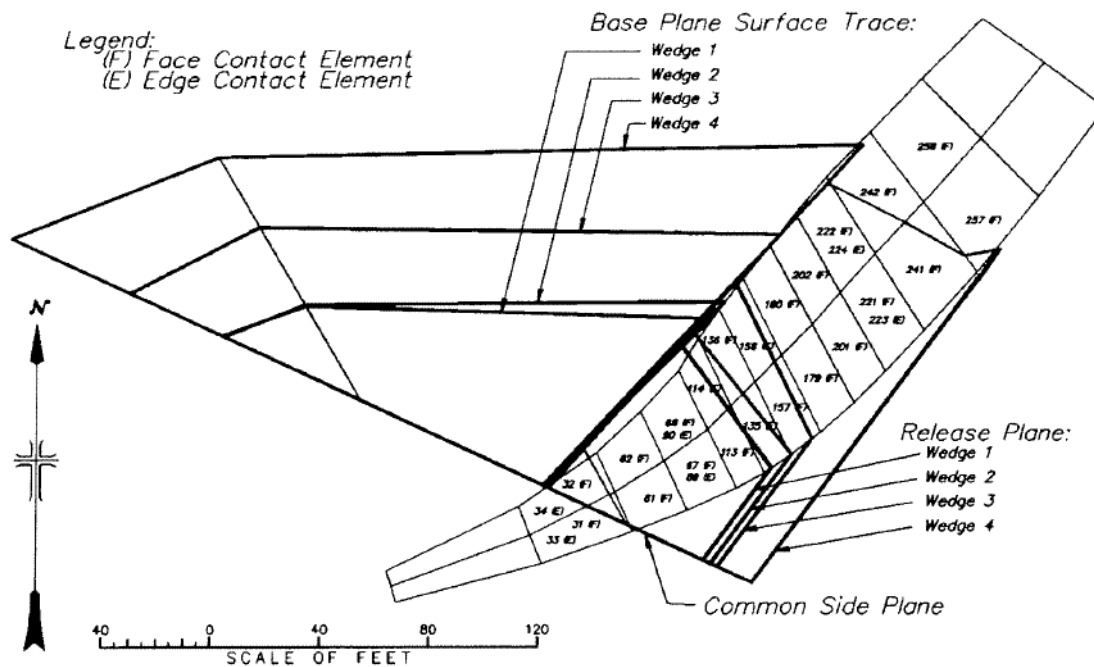


Figure D-7-10 Finite Element Mesh Superimposed on Nested Foundation Wedges

The foundation rock mass modulus used in such analyses can be an important consideration in a couple of regards. First, if there is significant differential foundation deformation between rock types with different deformation properties within the foundation of a concrete dam, severe cracking of the concrete, perhaps leading to adverse conditions that could cause dam rupture might occur. More typically considered, the foundation modulus affects how stresses are distributed within the dam structure and how load is transferred to the foundation wedges. In the case of dynamic loading, the extent of radiation damping is dependent on the foundation modulus values as well.

There are several ways to estimate foundation modulus. However, it is important to note that the rock mass modulus includes the effect of the jointing, fracturing, and other discontinuities. Therefore, the rock mass modulus is not the modulus measured on intact pieces of rock core in the laboratory. Similarly, the modulus measured using geophysical tools is typically not

appropriate because it is measured at a strain rate that is too fast and at strains that are too small to represent the loading of a concrete foundation.

The easiest way to estimate rock mass modulus for a concrete dam foundation involves the use of empirical correlations developed from large scale in-situ jacking test results and rock mechanics index properties. One such relationship is shown in Figure D-7-11, which correlates in situ modulus with Rock Mass Rating (RMR) developed by Bieniawski. RMR is a rock mass quality index that rates the rock mass according to (1) the intact rock strength (typically from lab testing or point load testing), (2) rock quality designation (RQD), (3) joint spacing, and (4) the condition of the joints (continuity, weathering, infilling, roughness) (see Scott(1999) for further details). A separate evaluation would be required for each major rock unit within the foundation of the dam and the effects on dam response evaluated.

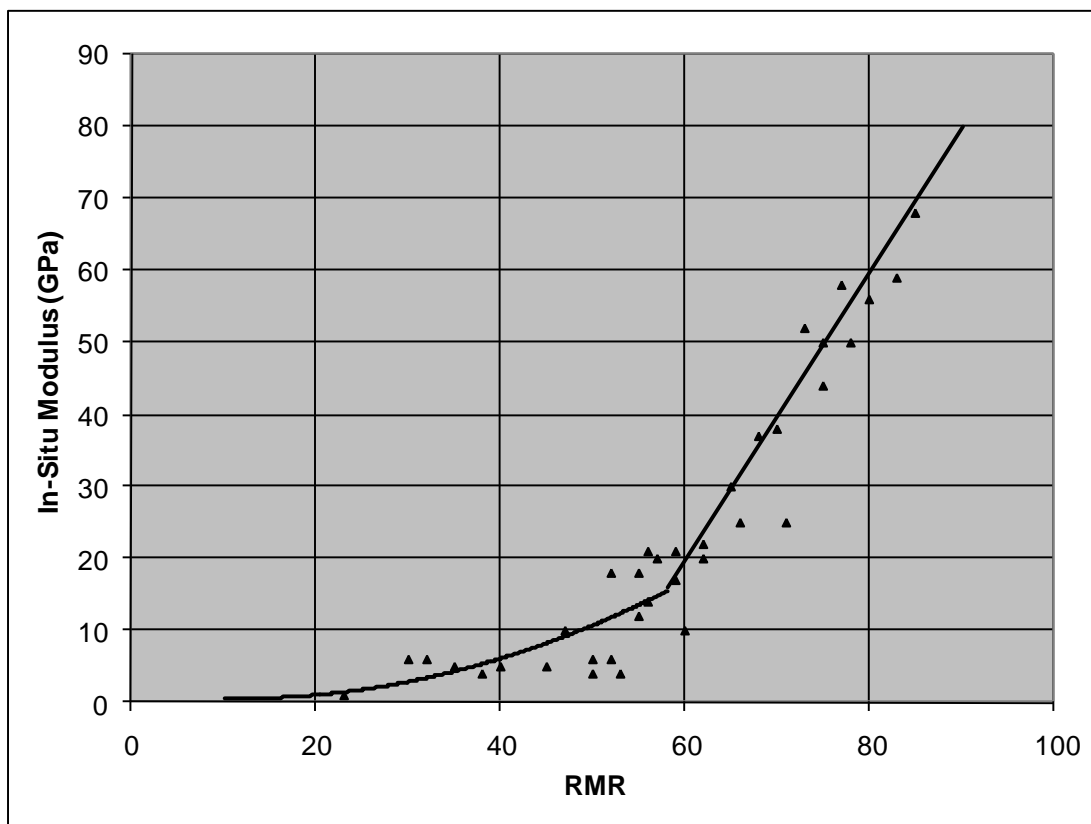


Figure D-7-11 Correlation between Rock Mass Modulus and RMR (adapted from Bieniawski, 1989)

It should be noted that there are other such empirical correlations, most of which include more scatter in the data (see Scott, 1999 for additional details). Therefore, when using empirical relationships, it is important to perform sensitivity studies to determine just how sensitive the results are to the values chosen, and to bracket the probable response of the dam and loading of the foundation.

In some cases the foundation rock may be anisotropic to a degree that requires modeling it as such. In that case it may be helpful to base the foundation modulus on the joint normal stiffness and spacing of the joints according to the equation $1/E_{rm} = 1/E_i + 1/K_n S$, where E_{rm} is the rock mass modulus, E_i is the modulus of the intact rock, K_n is the joint normal stiffness, and S is the joint spacing. This requires an estimate of the joint normal stiffnesses, probably through some laboratory testing. The modulus in different directions can be estimated using this approach. Scott (1999) provides some equations to account for jointing at different angles using this methodology.

The most direct way to estimate foundation rock mass modulus is to measure it using large scale jacking tests, such as that shown in Figure D-7-12. Loading is applied to the rock mass through large jacks or flat jacks, typically across an excavated tunnel or adit, and the deformation of the rock mass is measured at the rock surface and at depth beneath the loaded surface using multiple position borehole extensometer. The load and deformation data are then used to back calculate a modulus value for the given loading geometry. Limited equipment and expertise currently exists in the United States to perform this type of testing, and additional development may be needed to use this testing method in the future.

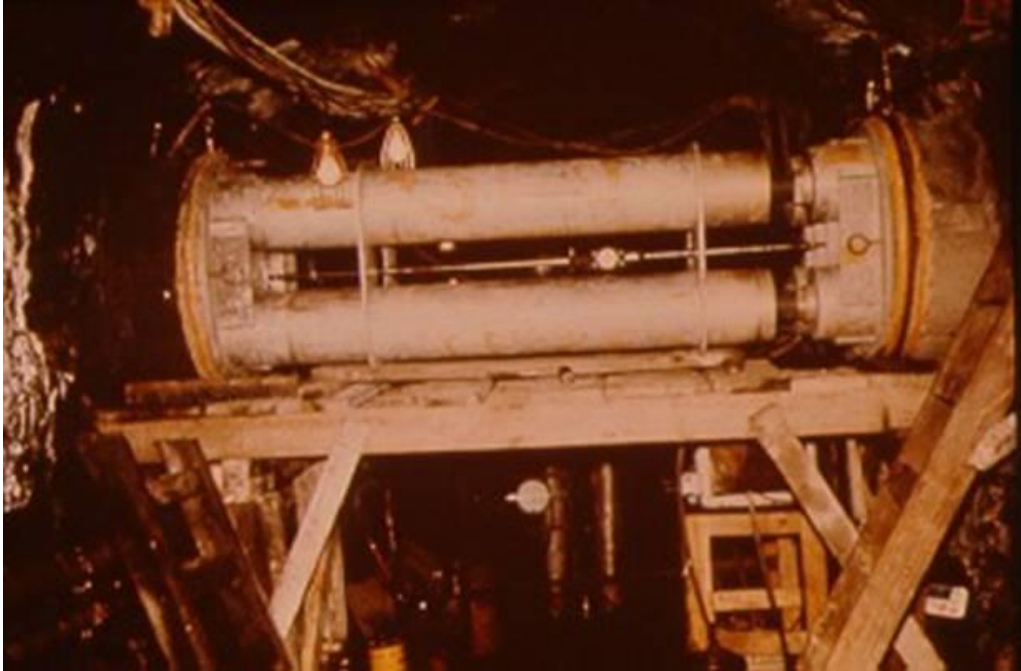


Figure D-7-12 In Situ Uniaxial Jacking Test Setup

Even though such a jacking test measures a relatively large volume of rock, it is small compared to the volume of a dam foundation. Therefore, a means of relating the jacking test results to the varying geologic conditions within the dam foundation must be established. One such method is seismic tomography. P-wave and/or S-wave velocities are measured over multiple overlapping ray paths between a series of source and receiver locations. The tomographic reconstruction process then gives a picture of the variation in velocity throughout the tested section, similar to a CaT scan. Figure D-7-13 shows a P-wave tomography developed for a dam abutment.

Receivers were placed in the roof of an exploratory adit, and sources were set off along a line on the abutment (ray paths between sources and receivers can also be developed between boreholes). As can be seen, there are zones of relatively large velocity contrast that may be important to the structural response and foundation loading.

A number of in-situ jacking tests were performed in the exploratory adit to correlate the P-wave velocities with modulus. The correlation was quite good, as shown in Figure D-7-14. Using this relationship, modulus values could be assigned to various velocity zones within the foundation, based on the seismic tomograms.

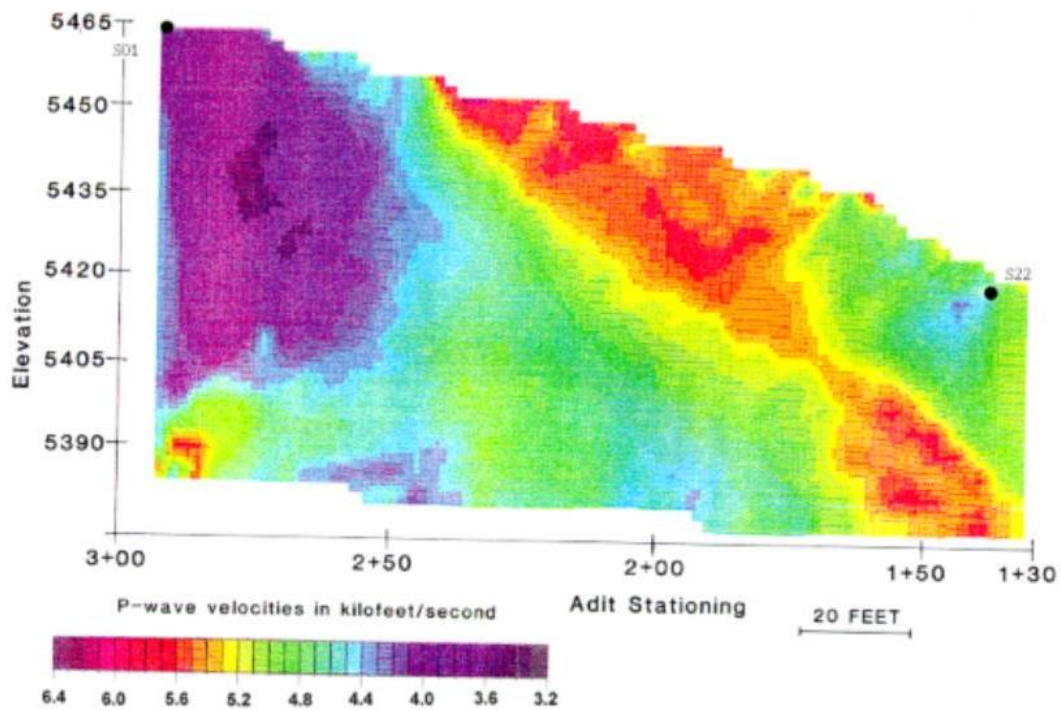


Figure A3. Seismic Velocity Tomogram Developed between Ground Surface and Adit.
 Note: 1000 ft/s = 305 m/s.

Figure D-7-13 Seismic Tomograph developed between Adit and Ground Surface

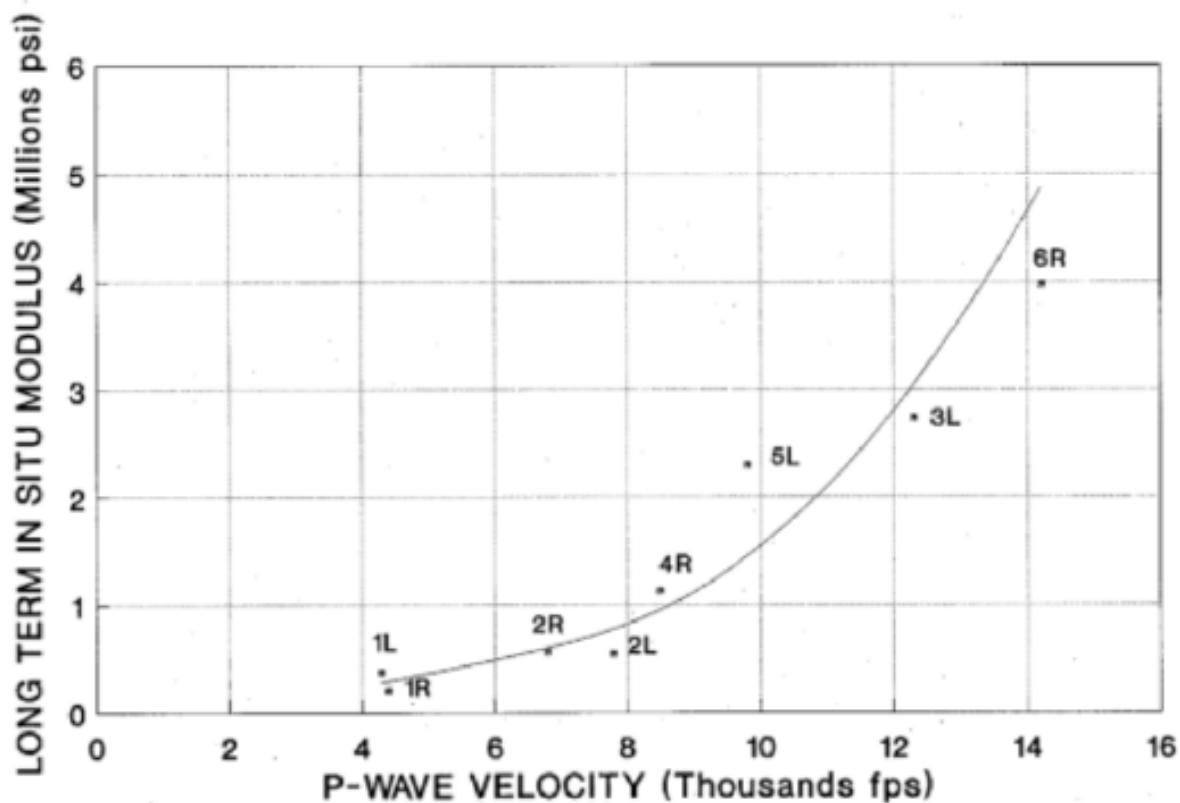


Figure D-7-14 Correlation of P-wave Velocity with In Situ Modulus

It should be noted that this is not the “Petit Seismique” method that relates rock mass modulus to the shear wave frequency. The Petit Seismique technique has found limited successful application in the United States.

So just how important is the foundation modulus for a concrete dam anyway? Table D-7-1 summarizes the Factor of Safety calculations for three foundation wedges beneath a thick arch dam, formed by upstream shallow dipping bedding base plane discontinuities, steeply downstream dipping back release joints, and near vertical continuous side joints. Uncoupled limit equilibrium sliding stability analyses were performed with dam loading calculated from three-dimensional finite element analyses. The only difference in the two cases summarized was the foundation modulus values. Case 1 represents a variable foundation modulus ranging from 0.6×10^6 lb/in² in the lower part of the foundation to 1.6×10^6 lb/in² in the upper part. Case 2 represents a similar distribution ranging from 1.5×10^6 lb/in² to 3.0×10^6 lb/in² (about twice as stiff). As can be seen, lower factors of safety were calculated for the stiffer foundation modulus

case. This is because the softer modulus allows the dam to deflect more, thus putting more of the load in arch action which in turn places more thrust against the side planes. Although the differences in this case are not large, such considerations could make a big difference if the factors of safety were lower, or when calculating probabilities of factors of safety less than 1.0.

Table D-7-1 Factor of Safety as a Function of Foundation Modulus

Modulus Case	Factor of Safety		
	Wedge D Left Abutment	Wedge E Channel Area	Wedge F Right Abutment
Case 1 (Soft)	2.8	2.1	3.2
Case 2 (Stiff)	2.1	1.9	2.3

When mass is included in the dynamic analysis of a concrete dam, the ratio of the concrete modulus to the foundation modulus can have a big influence on the radiation damping of the system. When the foundation modulus is small compared the concrete modulus, excessive radiation damping can result. Similarly, some programs use a reservoir bottom wave reflection coefficient (α) that is basically the fraction of the incoming waves that are reflected off the reservoir bottom. A low value of α can significantly reduce the response of the structure. Experience from eccentric mass shaking tests on concrete dams suggest that low empirically based foundation modulus values or low α values (less than about 0.8) can result in an over-damped model leading to unconservative results. Therefore, calibration of finite element models to shaking tests is recommended for critical dynamic analyses. The foundation modulus and other parameters are varied until the calculated natural frequencies match the measured frequencies.

A few final considerations for foundation modulus include the following:

- Little research is known to exist relative to the effect of grouting on foundation modulus. In-situ jacking tests were performed before and after grouting the affected rock mass at the Auburn Damsite in California, and at Davis Dam on the Colorado River. In both

cases, no appreciable increase in modulus was observed after grouting. This could be because point-to-point contacts along discontinuities control the rock deformation and are not affected by the grouting, or thinner grout mixes may have been used such that the modulus of the grout was soft relative to the rock mass.

- It is often desirable to use different foundation modulus values for static and dynamic loading, due to considerations described above. This may be difficult to achieve with some of the newer non-linear explicit finite element codes and may require load superposition.
- Typically softer foundation modulus values are not necessarily conservative. Sensitivity analyses are often warranted to evaluate the effect foundation modulus has on the results.
- A rock mass is often more deformable in tension. Therefore, if large tensile stresses are predicted near the heel of a dam, it may be appropriate to soften the foundation modulus in this area to account for opening of joints and discontinuities.

D-7.6 Two-Wedge Gravity Dam Analyses

Figure D-7-15 shows a two-wedge sliding analysis typically performed for concrete gravity dams, especially when founded on horizontally bedded sedimentary rock. The traditional 2-D analysis usually involves a passive wedge downstream of the dam. Although this type of analysis can be found in many guidance documents, it can be misused. For one thing, unless the passive wedge is very thin, the intact rock material is very weak, or there is an adversely oriented discontinuity or joint set passing through the passive wedge, it is unlikely that shearing will occur through the passive rock mass. In addition, in order for the passive wedge to move, shearing must occur along the boundary between the active and passive wedge. Unless there is a near vertical joint or discontinuity in this location, this may be unlikely. Finally, the calculated factor of safety is typically sensitive to the inclination angle assumed for the interwedge force, F . At the limit of equilibrium this should approach the friction angle of the interwedge plane. It is usually taken as horizontal which may be conservative in many cases.

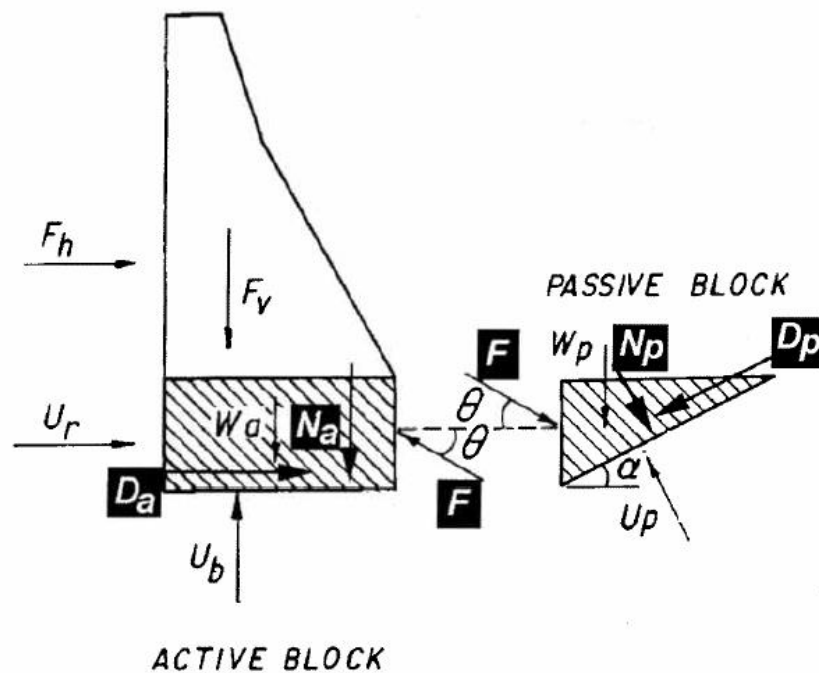


Figure D-7-15 Typical Two Wedge Sliding Analysis

Some deformation is typically needed to mobilize the passive wedge. If there are deformable discontinuities in the rock mass downstream, that deformation may lead to cracking of the concrete. Consider the roller-compacted concrete (RCC) gravity dam shown in Figure D-7-16. The dam is founded on a Cambrian quartzose sandstone foundation. In the abutments and beneath the main dam, interbeds of gray argillite, a lower strength material in between shale and slate, are present. Figure D-7-16 shows a typical instrumentation layout at Line C in the spillway area. Note that there is a weak layer, the Unit L argillite, within the otherwise hard quartzose sandstone. A passive wedge is present downstream of the dam above the Unit L layer. Of note are the vertical and angled MPBX's passing from the gallery through the dam and into the foundation, with anchors above and below the Unit L layer. Piezometers are also installed above and below the Unit L layer, and upstream and downstream of the line of drains. Not shown are the vertical inclinometers passing through the dam and into the foundation through the Unit L layer at sections outside the spillway.

Figure D-7-17 shows the response of the angled MBPX at line C during the first reservoir filling. As the reservoir went up, the anchors below the Unit L argillite layer began to deviate while those above did not. This meant that there was relative movement between the lower anchors and the anchor head, but not between the upper anchors and the anchor head. This suggested that the wedge above the Unit L was moving with respect to the rock below the Unit L. In addition, an inclinometer at a nearby location showed a distinct offset in its profile across the Unit L argillite layer. The piezometers showed relatively high pressures in the upstream and middle area of the foundation.

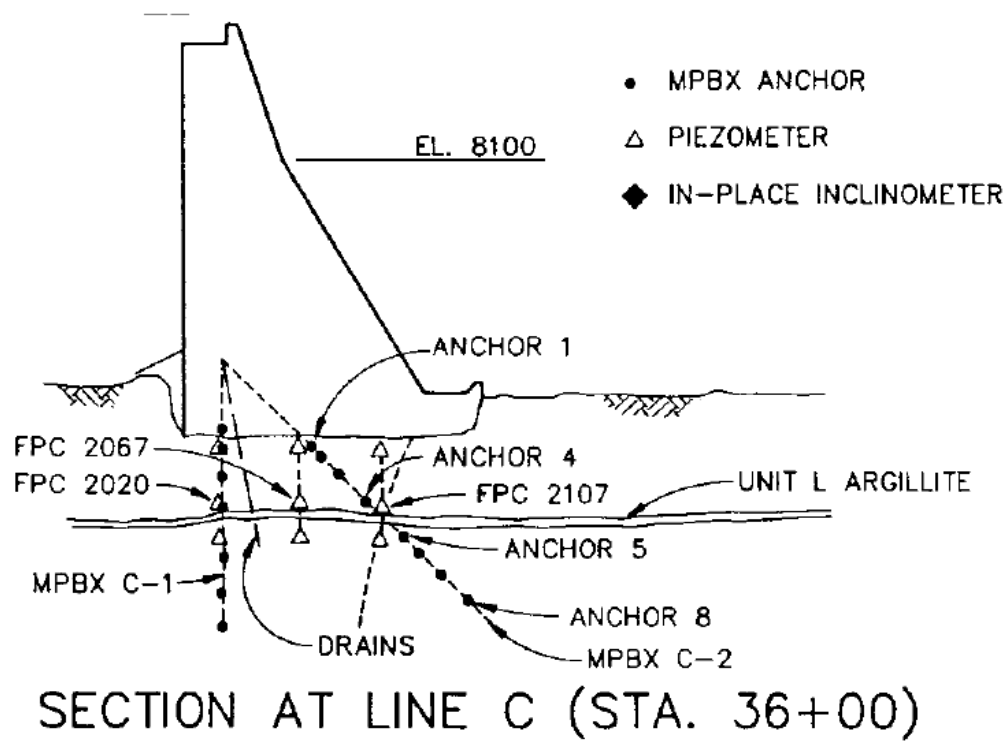


Figure D-7-16 Instrumentation and Geologic Section

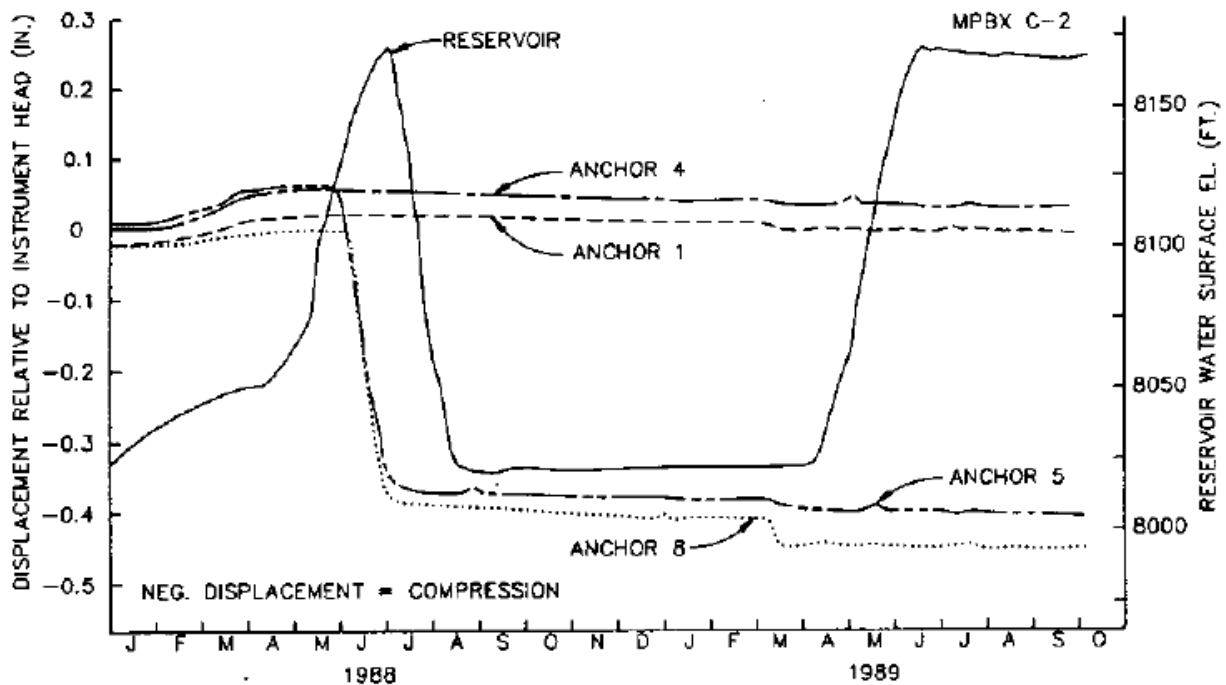


Figure D-7-17 Angled MPBX Response

Although movement was indicated, the decision was made to continue filling since it was concluded that failure was not in progress and the passive wedge was stable. This conclusion was reached because movement was occurring at a constant rate with increasing reservoir, and movement magnitude and direction was non-uniform across the site. Nevertheless, instrument readings were taken twice a day and sent to the designers for review. If there was any indication of accelerating movements, the designers were given the authority to stop the filling and start drawing down the reservoir. This never occurred, and the movement abruptly stopped when the reservoir filling stopped. The downstream passive resistance was being mobilized through closing of joints in the rock mass which allowed enough deformation to open existing thermally induced cracks. But since there was not an upstream dipping discontinuity, the movement stopped once the passive wedge was mobilized. It should be noted that the foundation movement was enough to open some thermally-induced cracks in the RCC to the point that remedial repairs were required.

A better approach to performing analysis of multi-wedge systems is to use a distinct element code such as Universal Distinct Element Code (UDEC) or a Discontinuous Deformation Analysis code (DDA), as shown in Figure D-7-18. This type of analysis accounts for the interwedge forces and angles more appropriately. But again, the failure planes must be realistically possible.

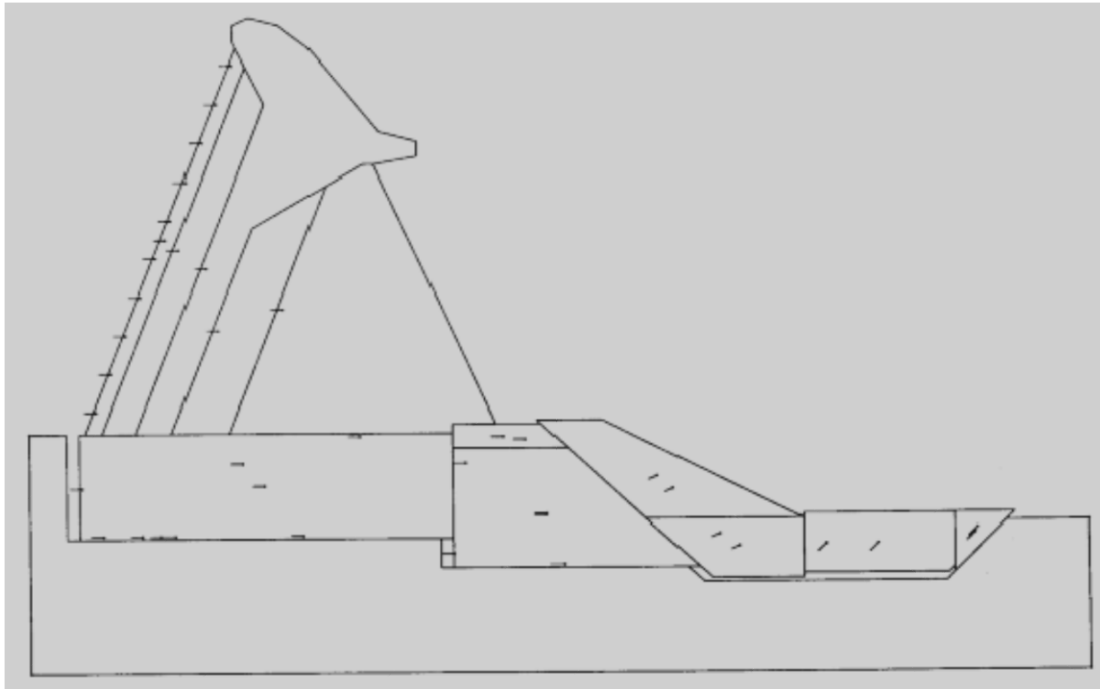


Figure D-7-18 DDA Analysis of Multi-Wedge System

D-7.7 Coupled Dam-Foundation Analysis

An uncoupled evaluation of foundation wedges with external dam loading is typically performed using stereographic vector analysis or rigid block analysis techniques. If these types of analyses indicate high risks, or large dynamic foundation wedge displacements, it may be useful to perform a nonlinear coupled analysis whereby the dam and foundation wedge are included in the same model, as shown in Figure D-7-19. This allows for stress redistribution and allows interaction between the dam and foundation. In addition, if the dam is very thick and it is thought that the potential for foundation wedge movement might be controlled by contraction joints within the dam, this type of analysis can be helpful in demonstrating this type of behavior. However, these types of analyses are complicated, time consuming and expensive, and mistakes

in model development can be made. Therefore, it is essential to thoroughly test the model to make sure it is performing correctly and giving reasonable results.

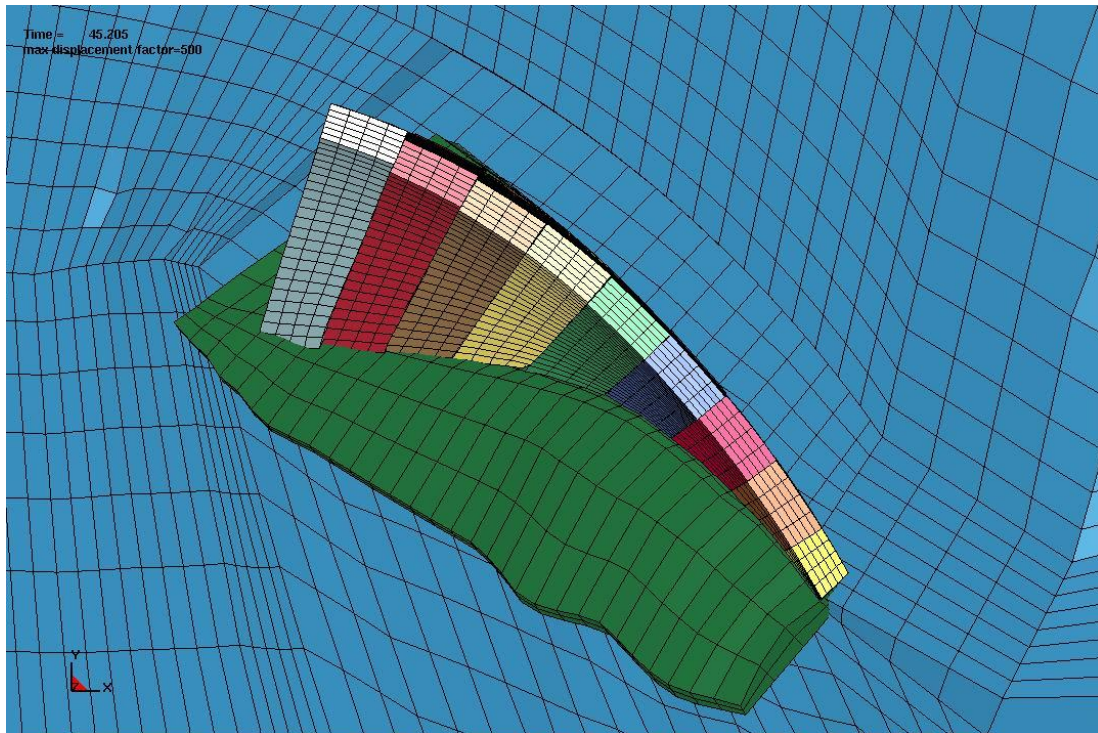


Figure D-7-19 Nonlinear Coupled Dam-Foundation Analysis

D-7.8 Example Concrete Dam Foundation Risk Analysis

An example of a potential failure mode description, as initially written and then as edited to be more useful is listed below (see also chapter on Potential Failure Modes).

- **Unedited** (insufficient detail): Sliding of the concrete dam foundation.
- **Edited:** As a result of high reservoir levels and continuing increase in uplift pressure in the right abutment of the arch dam due to inability to maintain the drainage system, and large earthquake shaking (the initiator), sliding of large rock Wedge No. 3 initiates. Wedge 3 is formed by (1) the continuous near vertical bedding plane parting seen downstream of the dam, (2) the continuous low angle joint seen downstream of the dam and in construction photographs crossing the foundation, and (3) the high angle joint sets mapped in the reservoir area trending cross canyon. The arch dam is unable to

angle joint can be observed in the downstream abutment, and construction photos indicate it traverses completely across the dam foundation forming the wedge base plane. Continuous high angle joints were mapped in the upstream reservoir area, capable of forming back release surfaces for the wedge.

- *It is not possible to maintain the foundation drainage system. The foundation drain holes were drilled from an upstream fillet and connected to the outfalls through piping with a series of right angle bends. It is not possible to maneuver drain cleaning equipment around these bends.*
- *The piezometer levels are increasing. Piezometers installed at the base of the dam indicate rising foundation water pressures. The pressures have risen 50 to 60 ft. near the lower right abutment since 1942.*
- *Water squirts up about 3 ft from rockbolt holes on the downstream right abutment. These rockbolt holes are downstream of the right abutment rock wedge and squirt when the reservoir reaches high elevations, indicating high foundation water pressures downstream of the dam.*
- *Analyses indicate Factors of Safety against sliding for the rock wedge drop below 1.0 for several excursions during earthquake ground motions representative of a M6.5 earthquake, 0.5g peak ground acceleration, annual maximum arch thrust, and currently estimated uplift conditions.*

D-7.10 Favorable or “Less Likely” Factors

- *The bedding plane parting side plane provides resistance since there is a component of the arch thrust acting normal to this discontinuity.*
- *There has been no indication of foundation movement to date. Although the collimation system is not set up to measure foundation movements on the right abutment, there is no indication of offset joints or concrete cracking in the area of the right abutment wedge.*
- *Analyses indicate static load Factors of Safety exceeding 1.5 for currently estimated uplift conditions and maximum annual static arch loading conditions with frictional strength only (no cohesion) based on sliding tilt tests (45 degrees on the side bedding plane parting and 50 degrees on the rougher base plane joint).*

The semi-quantitative risk screening and rationale might look something like the following (see also chapter on Semi-Quantitative Risk Analysis):

Likelihood rating: Moderate to High; Available earthquake analyses suggest large earthquake ground motions with an exceedance probability slightly more remote than 1/10,000 could trigger movement of the wedge under currently estimated water pressure conditions. It is unknown whether ground motions more frequent than 1/10,000 would also trigger wedge movement. Additional key evidence is weighted toward “more likely” as follows: foundation water pressures continue to rise, reducing stability, the foundation drains cannot be cleaned due to numerous right angle bends in the embedded connecting piping, and evidence of high pressures in the abutment includes water squirting from rockbolt holes at high reservoir levels.

Likelihood confidence rating: High; the evidence is clear that water pressures are increasing and sufficient analyses have been performed to indicate potential behavior of the abutment wedge under increased seismic loading. It is unlikely that additional information would change the category significantly. However, analyses at other ground motion levels and a detailed quantitative risk analysis may provide additional insights into remediation alternatives and better information from which to make a decision.

Consequences rating: Level 3; although only the top portion of the dam would breach, it is expected that such a failure would be rapid and brittle, with a wall of water over 60 feet high initially traveling down the canyon. Most of the reservoir volume is contained in the upper third of the reservoir. Approximately 60-80 people in the 40 km of valley between the dam and State Highway 52 (including those in 30 cabins, the Sunrise Resort, the Gold Gulch campground, and 6 ranches, all of which are located near the river) could be caught by surprise and the fatality rate is expected to be high in this reach. There are no towns or settlements for the next 50 km, then four smaller towns will be inundated before the flood hits a larger town about 150 km downstream, with over 10,000 people estimated at risk in these communities. The warning time in these downstream communities should keep the fatality rate low, although some fatalities would be expected, especially if failure occurred at night.

Consequences Confidence Rating: High; a high level reconnaissance was performed to evaluate the population at risk, and given the small warning time and deep, rapid flooding near the dam, it is unlikely that additional information would change the rating. However, it would be valuable to further quantify the consequences if a quantitative risk analysis is performed.

This semi-quantitative evaluation plots on the risk matrix as shown in Figure D-7-21. Based on the fact that the risks plot with high confidence in an area on the matrix where they may justify action, a quantitative analysis of risk for this potential failure mode can be justified. Given the detailed description of the potential failure mode, an event tree can be constructed as shown in Figure D-7-22. Only one seismic load branch (1/10,000 to 1/25,000 annual exceedance probability) is constructed all the way through the event tree for illustration purposes. The conditional failure probability branches following the load branch must be duplicated for all load ranges above the threshold load value. The probability of failure is dependent on not only the earthquake loading level, but also the reservoir level at the time the earthquake hits. If several reservoir and earthquake levels were represented in the tree, it would be extremely large. To simplify the evaluation, only one reservoir load range was included, chosen to represent loadings which were significant to the abutment wedge and at levels that would produce significant consequences if failure occurred. The event tree was developed after a credible foundation wedge had been defined based on a detailed evaluation, and the primary geologic uncertainty is the joint continuity. Uncertainties related to joint orientation, strength, and water forces for a given uplift condition do not necessarily follow linearly, are interrelated, and all affect the stability. These were handled in external kinematic stability analyses as discussed below.

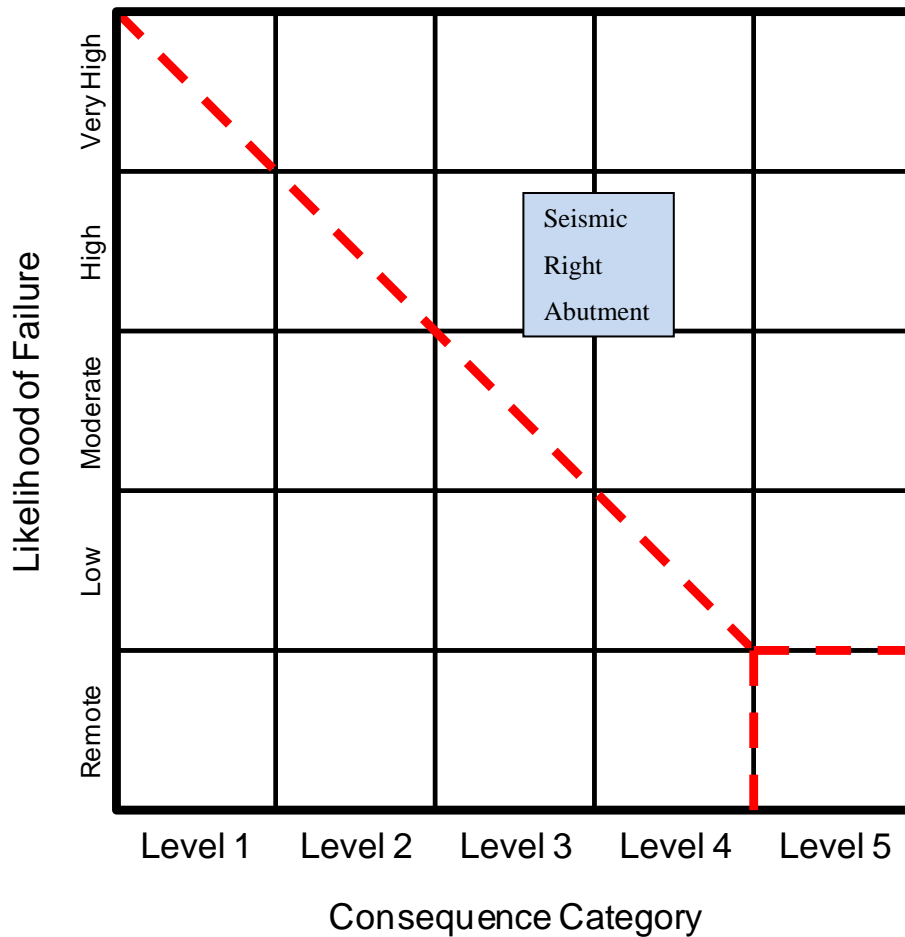


Figure D-7-21 Risk Matrix

Probabilities for the reservoir and seismic load ranges were taken from exceedance probability hazard curves (see relevant chapters in this manual). All other branch probabilities, with the exception of post-earthquake breach, were based on subjective expert elicitation as discussed below (see also associated chapter in this manual) after the appropriate risk team members had a chance to review and discuss a number of three-dimensional uncoupled dynamic analyses of the foundation for various seismic loadings and input parameters.

To examine the post-earthquake stability of the wedge (assuming it survived the earthquake shaking), the standard deterministic equations for calculating the three-dimensional factor of safety against sliding (Hendron et al 1980) were programmed into a spreadsheet. Distributions were input for the variables as described below, and the spreadsheet was used to perform a

Monte-Carlo analysis to determine the probability that the factor of safety against sliding was less than 1.0, as described in the chapter on Probabilistic Stability Analysis. For stability analysis purposes, dip, dip direction, and effective friction angles of the discontinuities forming the abutment wedge are uncertain. The orientation of the bedding is more regular and better defined than the other joints. Therefore, the dip and dip direction of the bedding were defined as a triangular distribution (low value, best estimate value, and high value) with the mean measured value representing the peak of the distribution, plus and minus three degrees to define the maximum and minimum values. Similar distributions were defined for the other joint sets, except that one or two additional degrees were added and subtracted to define the upper and lower limits.

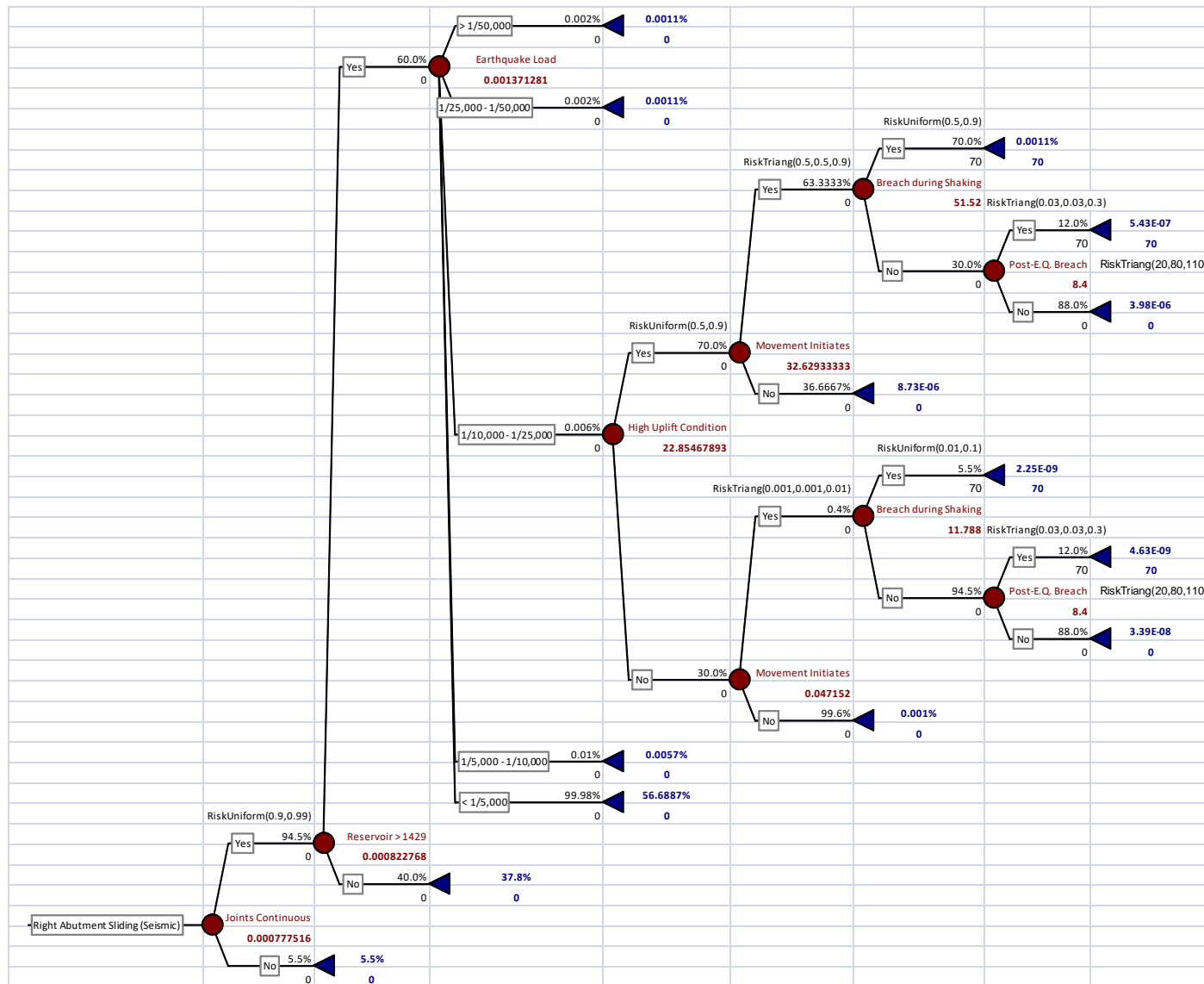


Figure D-7-22 Example Event Tree

In the case of effective friction angles, enough tilt tests were performed on large bedding joint specimens, that a mean and standard deviation (following approximately a normal distribution) could be defined from the results. However, a smaller standard deviation was actually used since it was thought many of the low and high strength samples would represent only localized areas of the plane and not the overall effective strength of the entire surface. Since the other joints appeared to be rougher, both the mean friction angles and standard deviation were increased by a few degrees compared to the bedding joints.

The weight of the wedge was varied in the analysis using a uniform distribution (equally likely between lower and upper input values) considering reasonable variations in unit weight and wedge volume. The water forces are also uncertain, but for post-earthquake conditions it was assumed the joints opened sufficiently to generate full hydrostatic loading on the back release joint, varying linearly to the “daylight” trace of the side and base plane joints downstream. The post-earthquake thrust from the arch dam, although uncertain, was taken as constant for a high reservoir elevation, based on finite element structural analyses simulating post-earthquake conditions to the extent possible. The results of 10,000 iterations in terms of sliding factor of safety are shown in Figure D-7-23. As can be seen, approximately 2.9 percent of the calculated factors of safety were less than 1.0 (i.e. probability of $FS < 1.0 = 0.029$).

Enough information did not exist to define the analysis input distributions with extreme confidence. Therefore, a key component to performing the probabilistic analysis was examining which input distributions had the largest effect on the output safety factor distribution. For this, the @Risk program prints out a list of ranking coefficients. Those input distributions with the highest positive or negative ranking coefficients affect the results most. The coefficients for this analysis are shown in Table D-7-2.

The larger the absolute value of the coefficient, the greater the effect of that parameter on the results. A negative ranking coefficient just means that the variable is negatively correlated with the result. That is, an increase in the parameter results in a decrease in the factor of safety. It can be seen that the base plane effective friction angle affects the results the most followed by the side plane dip direction. The side plane friction angle and base plane dip also have a relatively significant effect on the results. For those parameters with the highest ranking coefficients,

additional parametric studies were appropriate to examine how a small change in the distribution affects the results. If the mean value of the four most sensitive parameters is changed by two degrees in the negative direction, and the limits and standard deviations are increased by two degrees, the probability of $SF < 1.0$ increases by about an order of magnitude to 32.8 percent. This was considered to be the upper bound of a triangular distribution, whereas the mean value (2.9 percent) was taken as the lower end and best estimate of the distribution.

Three of the event tree nodes were estimated using subjective degree-of-belief methods: Joints Continuous, High Uplift Condition, and Breach during Shaking. To illustrate the process that was used, only the “High Uplift Condition” node will be described here. For this node, the team estimated the likelihood that the high water pressures represented by a pressure contour map developed by the rock mechanics analyst was truly representative of what exists in the abutment, or whether there was enough residual drainage in the system and natural jointing to be more typical of what one would expect of a drained abutment. The adverse and favorable factors related to this node are listed below. Note that some are the same as originally used in the failure mode screening, and that some of the factors provide opposing views on a given condition. This will often be the case, and the team must decide which of the factors are most convincing.

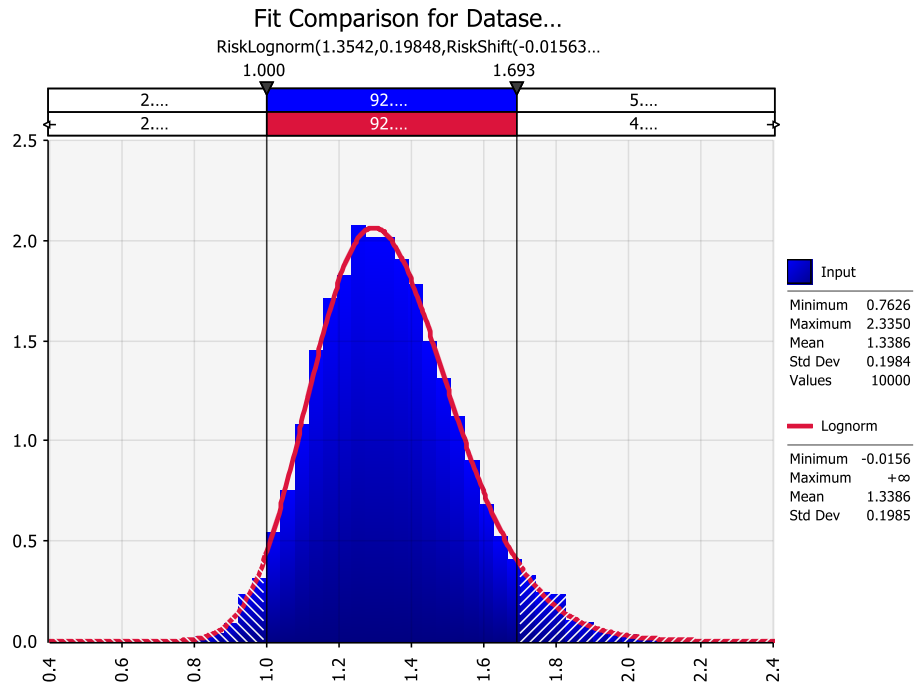


Figure D-7-23 Output from Monte Carlo Simulation (horizontal axis is factor of safety)

Table D-7-2 Sensitivity Rank Coefficients

Parameter	Spreadsheet Cell	Regression Coefficient
Joint set 3 dip direction (CW w/r N), Back	B22	0.058
Joint set 2 dip direction (CW w/r N), Side	B21	-0.527
Joint set 1 dip direction (CW w/r N), Base	B20	0.154
Dip of joint set 3 (degrees), Back	B17	0.019
Dip of joint set 2 (degrees), Side	B16	0.048
Dip of joint set 1 (degrees), Base	B15	-0.333
Estimated weight of the wedge	C9	0.044
f3, the Joint Set 3 friction angle, Back	B37	0
f2, the Joint Set 2 friction angle, Side	B36	0.367
f1, the Joint Set 1 friction angle, Base	B35	0.648

D-7.11 Adverse or “More Likely” Factors

- It is not possible to maintain the foundation drainage system. *The foundation drain holes were drilled from an upstream fillet and connected to the outfalls through piping with a series of right angle bends. It is not possible to maneuver drain cleaning equipment around these bends.*
- The piezometer levels are increasing. *Piezometers installed at the base of the dam indicate rising foundation water pressures. The pressures have risen 50 to 60 ft. near the lower right abutment since 1942.*
- Water squirts up about 3 ft. from rockbolt holes on the downstream right abutment. *These rockbolt holes are downstream of the right abutment rock wedge and squirt when the reservoir reaches high elevations, indicating potentially high foundation water pressures well downstream of the dam.*

D-7.12 Favorable or “Less Likely” Factors

- The water pressure contours used in the analysis show levels above the ground surface downstream of the dam in areas where no seepage appears.
- The rockbolt holes that squirt water are downstream of the rock wedge. *The pressures under the wedge are not known; it may be that the water is connected to the rockbolt holes through a path that does not feed the wedge planes. It is not clear if the rockbolt holes squirted when the drainage system was new.*
- The piezometers that show increasing pressures are not in the vicinity of the rock wedge. *The closest piezometer is at the base of the right abutment; the wedge is in the upper right abutment. There are no piezometric measurements under the rock wedge.*

The team weighed the evidence and decided on a low estimate of neutral (0.5) and a high estimate of likely (0.9) for high water pressures existing in the abutment consistent with the analysis, with no reason to believe it is more likely anywhere within the range (i.e. a uniform distribution). The rationale is as follows: there is clear evidence that the original drainage system is deteriorating and cannot be maintained, and there is evidence that water pressures in the abutment could be high at higher reservoir elevations. Therefore, estimates on the likely side are

warranted. The primary mitigating factor that keeps the estimates from being higher is the fact that there are no piezometric measurements to confirm the values used in the analysis, which may be at least locally on the conservative side as indicated by localized estimated levels above the ground surface.

The consequences study will not be described in detail here. However, suffice it to say that, although there were some fatalities estimated at towns downstream where the valley widens, most of the consequences resulted from high severity flooding along the narrow canyon downstream of the dam where the population at risk is about 60-80 in scattered residences, campgrounds, and resort areas. Due to the expected sudden rupture of the dam associated with the foundation sliding potential failure mode, it is expected there would be minimal warning in this reach.

Monte-Carlo simulation results developed from the event tree shown in Figure D-7-22 are depicted in the scatter-plot shown in Figure D-7-24, where each point represents a single combination of possible values chosen from each variable's probability distribution. The mean (shown by the large open circle) represents the 'expected value' of the risk estimates (where the weighted consequences are typically calculated as the annualized life loss divided by the annualized failure probability). The outlying points represent situations where more extreme values are chosen from each variable's probability distribution. The likelihood of and extent to which the variation in results exceed the risk guidelines (in this case Reclamation's guidelines shown) can be an important input to the decision process.

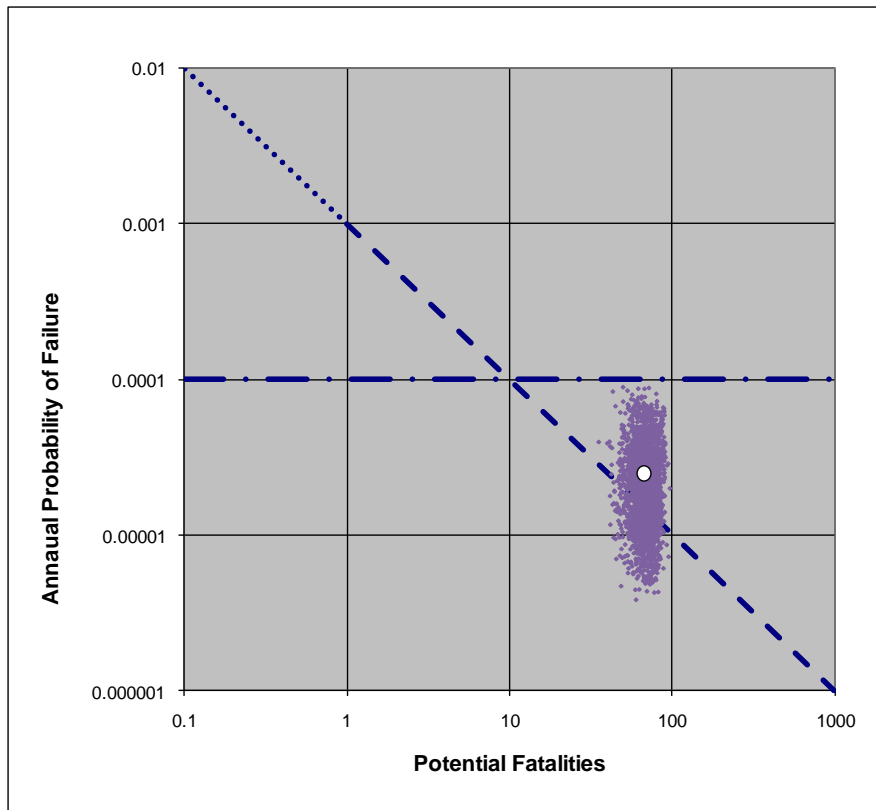


Figure D-7-24 Scatter Plot from Event Tree Monte-Carlo Analysis

Comparing Figure D-7-24 with Figure D-7-21 indicates that the risks are estimated to be slightly lower from the detailed quantitative risk analysis in comparison to the semi-quantitative screening. Although the consequences category was a reasonable reflection of the detailed evaluation, the likelihood category was about half an order of magnitude higher than the quantitative estimates.

For this example, a detailed evaluation of the complete event tree indicates the following (listed here to give a flavor for the types of information that can and should be gleaned from such an exercise):

- No one seismic load range dominates the risk. The decrease in load probability roughly offsets the increase in conditional failure probability as the loading increases.
- The risk is dominated by the branches corresponding to high uplift pressures. If it could be assured that the abutment was well drained and the chance of high uplift pressures was

negligible, the mean estimated annualized failure probability would drop from about 2.1×10^{-5} to 1.5×10^{-6} . (Note: event trees provide a useful tool to examine the effects of potential risk reduction actions that would alter the estimated probabilities for one or more branches.)

- In general, the risk is dominated by dam failure as a result of abutment wedge movement during seismic shaking (as opposed to post-earthquake conditions). Even in cases where dam failure during seismic shaking was thought to be unlikely, the probability of post-seismic instability was even more unlikely. The exception was the seismic load range from 1/10,000 to 1/25,000 and drained conditions where the chance of failure during seismic shaking was estimated to be very low. (Note: the chance of failure was considered to be negligible for 1/5,000 to 1/10,000 ground motions and drained conditions.)
- The mean risk for this one potential failure mode exceeds the public protection societal risk guideline of 0.001 lives per year, plotting in the area of increasing justification to reduce or better understand the risks (although none of the simulation points exceeded the 0.0001 annualized failure probability threshold). It therefore follows that the total risk (sum of all potential failure modes) will also exceed the risk assessment guidelines

Building the case requires establishing claims and the evidence to support the claims. In this case one of the claims is that the seismic hazard curve appropriately represents the probability of seismic loading at the site. The evidence to support this claim includes careful evaluation of potential seismic sources which include north- to northwest-striking Cenozoic normal faults with known or possible Quaternary displacement, and random or background seismicity on buried faults that lack surface expression. One nearby range-bounding fault shows clear evidence of late Quaternary displacements from observations of offset soil profiles, and the fault lengths and slip rates could be reasonably deduced from the exposures. Observations at other range-bounding faults were hampered by access problems, extensive vegetation, and obliteration of the record by erosion. However, even if they are treated the same as the fault with observed late Quaternary displacement, the inferred slip rates are low enough that the seismic hazard is clearly dominated by the background seismicity. The historic earthquake record in the vicinity of the dam is good, with instrumented recordings extending back to 1925. A total of 223 earthquakes

were available for recurrence calculations, with two greater than M 6.5. Earthquake recurrence statistics show that the data follow a “maximum likelihood” fit quite well. Therefore, confidence in the predictive capability of the recurrence model is reasonably high.

Several claims are made in evaluating the event tree in support of the overall claim that the chances of poor abutment performance under seismic loading are higher than we would like to see for the associated consequence level. The first claim is that the upper right portion of the dam is founded on a well-defined foundation wedge, formed by continuous bedding plane partings and joints, with the probability of the joints being continuous enough to allow release of the wedge estimated to be high (0.9 to 0.99). The evidence to support this claim includes the following: (1) a continuous open bedding plane parting forming the side plane of the wedge was mapped downstream of the dam, (2) a continuous open low angle joint forming the base plane of the wedge was mapped downstream, (3) a construction photograph indicates the base plane is continuous across the foundation contact to the upstream side of the dam, and (4) joints mapped upstream of the dam could connect to form a continuous release surface at the back of the wedge.

The second claim is that there is a good chance that high water pressures exist within the right abutment near the wedge. The evidence to support this claim includes the following discussion. The foundation drainage system cannot be cleaned or maintained as evidenced by the way in which it was constructed with numerous right angle bends between the drain holes and the outfalls. Although there are no direct measurements of abutment water pressures in the immediate vicinity of the right abutment wedge, evidence suggesting the foundation water pressures are increasing and may be high in the vicinity of the wedge (with an estimated probability from neutral to likely, 0.5 to 0.9) includes: (1) piezometric pressures measured at the base of the right abutment have increased by over 45 ft. since 1947, and (2) rock bolt holes immediately downstream of the wedge squirt water about 3 ft. into the air at high reservoir levels.

Given this information, detailed deterministic and probabilistic analyses were performed to estimate the probability of the remaining nodes under various earthquake load ranges and abutment water pressure conditions. Additional details of the analyses and results, why they are

believable, and how they were weighted to arrive at probability estimates were also provided in building the case.

The claim relative to consequences is that there would be multiple fatalities if this potential failure mode were to develop, most likely in the range of 50 to 80. Evidence suggests the type of breach that would result from concrete arch dam abutment instability would be rapid and brittle, based on historical experience such as the sudden failures of St. Francis Dam in southern California and Malpasset Dam in southern France. Given such a failure, a wall of water over 60 feet high would travel down the canyon downstream of the dam. The approximately 60-80 people (on average) in this portion of the canyon in cabins, campgrounds, resorts, and ranches who reside primarily near the river would be subjected to high severity flooding with no warning other than the seismic ground vibrations and sound of the rushing water. Nearly 80 percent of the total fatalities are estimated to occur in this reach. Once the flood wave exits the canyon, it would spread out and attenuate. Several small towns and a large town would be affected by the flooding, particularly those people nearest the river. Although fatalities are expected in these areas, the reduced flood severity and warning will keep them to about 20 percent of the total.

The evidence was compelling that risks were in an area of increasing justification to reduce risks, and confidence in the evaluation high enough that decision-makers were convinced to take action. In this case, a drain drilling program for the right abutment was proposed. Assuming a drain drilling program would be effective in reducing abutment water pressures and increasing stability, the annualized failure probability was first evaluated by setting the probability of “High Uplift Condition” to zero in the event tree, resulting in an estimated reduction in risk of just over an order of magnitude. The chances of achieving this condition were thought to be good, which resulted in moving forward with a drain-drilling program for the right abutment.

The risks associated with introducing drill water into the wedge potential sliding planes during drain or piezometer drilling and triggering a sliding situation were evaluated. Given the currently relatively high static factors of safety, the localized effect of the drill water pressure injection, the fact that the drilling would mostly occur at a time in the late spring when the reservoir was being drawn down for water supply, and the fact that the drains would be drilled from a rock face lower on the abutment from which it would not be possible to charge the rock

joints with a significant column of water pressure, it was determined that the increase in risk during drain drilling was very small.

Piezometers installed in the vicinity of the abutment wedge planes prior to drilling the drains confirmed that the pre-drainage abutment water pressures were elevated, and demonstrated the reduction achieved by the additional drainage as the drains were installed. A post-construction evaluation confirmed that the risks had been reduced by over an order of magnitude by the drain drilling program.

D-7.13 Relevant Case Histories

D-7.13.1 St. Francis Dam: 1928

St. Francis Dam was a curved concrete gravity dam constructed in San Francisquito Canyon approximately 45 miles north of Los Angeles California. The dam was 205 feet high, 16 feet thick at the crest, and 175 feet thick at the base. The crest length of the main dam was about 700 feet. The dam had no contraction joints or inspection gallery. The foundation was not pressure grouted, and shallow drainage was installed only under the center section. The foundation was composed of two types of rock; the canyon floor and left abutment were composed of relatively uniform mica schist, with the foliation planes dipping toward the canyon at about 35 degrees. The upper portion of the right abutment was composed of a red conglomerate, separated from the schist by a fault dipping about 35 degrees into the right abutment.

During reservoir filling, two sets of cracks appeared on the face of the dam that were dismissed as a natural result of concrete curing. The reservoir stood within 3 inches of the overflow spillway crest for 5 days before the failure. Large tension cracks were noted in the schist on the left abutment two days before the failure. The morning of the failure, muddy water was reported to be leaking from the right abutment, but when examined in detail, the flow was found to be clear, picking up sediment only as it ran down the abutment. Another leak on the left abutment was similarly dismissed as normal leakage. Several hours before failure the reservoir gage recorded a sudden 3.6 inch drop in the reservoir level. One of the caretakers was seen on the crest of the dam about an hour before failure. Several people drove by the dam just minutes before failure. One person reported crossing a 12-inch-high scarp across the roadway upstream of the dam.

The dam failed suddenly at 11:58 p.m. on March 12, 1928, as evidenced by the time the Southern California Edison power line downstream was broken. Within 70 minutes, the entire 38,000 acre-foot reservoir was drained. An immense wall of water devastated the river channel for 54 miles to the Pacific Ocean. It has been estimated that 470 lives were lost, but the exact count will never be known (Anderson et al, 1998). Reanalysis of the disaster indicated that failure initiated by sliding along weak foliation planes in the left abutment, perhaps on a remnant of an old paleo-landslide.

D-7.13.2 Malpasset Dam: 1959

Malpasset Dam was a 216-foot-high thin concrete arch structure completed in 1954 in southern France. The dam was 5 feet thick at the crest and 22 feet thick at the base. Blanket grouting was performed at the dam-foundation contact, but no grout curtain or drainage was installed, and no instrumentation other than survey monuments was provided. The dam was founded on gneiss. The reservoir filled for the first time on December 2, 1959. Although earlier there had been some clear seepage noted on the right abutment and a few cracks had been observed in the concrete apron at the toe of the dam, engineers visiting the site on December 2 did not notice anything unusual. About 9:10 p.m. that evening, the dam tender heard a loud cracking sound and the windows and doors of his house, on a hillside about 1 mile downstream of the dam, blew out. The sudden failure sent a flood wave down the river causing total destruction along a 7 mile course to the Mediterranean Sea. The number of deaths resulting from the failure was reported to be 421.

The failure was attributed to sliding of a large wedge of rock in the left abutment of the dam formed by an upstream dipping fault on the downstream side, and a foliation shear on the upstream side. The “mold” left by removal of the wedge could be clearly seen following the failure. Large uplift pressures were needed on the upstream shear in order to explain the failure. Experiments suggested that the arch thrust acting parallel to the foliation decreased the permeability perpendicular to the foliation to the point where large uplift pressures could have built up behind a sort of underground dam. The uplift forces in combination with the dam thrust were sufficient to cause the wedge to slide, taking the dam with it (Anderson et al 1998).

D-7.13.3 Austin (Bayless) Dam: 1911

Austin Dam was a concrete gravity dam about 43 feet high and 534 feet long constructed by the Bayless Pulp and Paper Company about 1½ miles upstream of the town of Austin, Pennsylvania. A four-foot-thick by four-foot-deep concrete shear key was constructed into the horizontally bedded sandstone with interbedded weak shale layers. Anchor bars were grouted 5 to 8 feet into the foundation, extending well up into the dam body, on 2-foot 8-inch centers, located at about 6 feet from the upstream face. No drains were provided for the dam or foundation. During initial reservoir filling in 1910, the center portion of the dam at the overflow spillway section slid downstream about 18 inches at the base and 31 inches at the crest. The reservoir was lowered, but no repairs were made and the dam was put back into service. As the reservoir filled again, the dam suddenly gave way on September 30, 1911. More than 75 people lost their lives in Austin. Back analysis suggests that sliding occurred on a weak shale layer within the foundation (Anderson et al, 1998).

D-7.13.4 Camara Dam: 2004

Camara Dam was a 160-foot-high roller compacted concrete (RCC) gravity structure with a downstream slope of 0.8(H):1(V) constructed in Brazil in the early 2000's. The dam was originally designed as an embankment dam, but was switched to RCC after the bulk of the exploration was completed. A gallery was constructed within the dam from which single line grout and drainage curtains were constructed. The dam was founded on gneissic migmatites with foliation dipping 30 to 35 degrees toward the right abutment. A "soil pocket" was discovered on the lower left abutment, which was excavated and filled with concrete. In reality, the soil was part of a major shear zone parallel to the foliation underlying most of the left abutment. Its extent was apparently missed due to the use of percussion exploratory drill holes, failure to understand that it locally pinched to smaller thicknesses, and failure to portray all the exploratory data on interpretive geologic plans and cross sections. There had been heavy rains in late January and early February of 2004 that filled the reservoir to within about 5 m or 15 feet of its maximum level. The reservoir continued to fill more slowly from that point into June. During that period of time, a crack in the gallery, heavy drain flows carrying soil material into the gallery, plugging of several drain holes, and emergence of a wet spot at the toe of the dam on

the left abutment were reported. At one point a recommendation was made to lower the pool but it went unheeded. It is not clear how fast the reservoir could have been lowered.

The dam failed on June 17, 2004. A portion of the foundation and dam was missing from the middle of the left abutment and the dam arched over the remaining void. This is unusual and indicates that stresses were redistributed around the unstable area, but the dam in that area was not strong enough to buttress the foundation. The smooth and relatively unfractured footwall of the shear was exposed on the left abutment, and its continuation above the breach could be seen. It is evident that there had to be some movement of the dam downstream and toward the channel to release the foundation wedge located above the shear. Professor Milton Assisi Kanji postulated that the shear zone was filled with pervious fill and the surrounding rock was relatively free of fracturing such that flow was confined along the shear zone. Plugging of the drains reduced the drainage capacity of the zone, and therefore seepage and uplift pressures developed along the zone well downstream of the toe of the dam. This large uplift pressure was enough to reduce the effective stress to the point where sliding occurred along the shear zone, taking a good portion of the dam with it. Erosion of the soil material from within the shear zone may have contributed to the failure, although it is not clear exactly how this would have manifest. It is possible the downstream portion of the wedge slid toward the channel first, removing the passive wedge. Five deaths were reported, 800 people became homeless, and extensive property and environmental damage resulted from the dam failure.

D-7.14 References

Anderson, C., C. Mohorovic, L. Mogck, B. Cohen, G. Scott, "Concrete Dams Case Histories of Failures and Nonfailures with Back Calculations," Report DSO-98-005, Bureau of Reclamation, Denver, Colorado, December 1998.

Bandis, S.C., A.C. Lumsden, and N.R. Barton, "Fundamentals of Rock Joint Deformation," Int. J. Rock Mech. Min. Sci. & Geomech. Abstr., vol 20, pp. 248-268, 1983.

Bieniawski, Z.T., Engineering Rock Mass Classifications, John Wiley and Sons, Inc. pp. 51-72, 1989.

Hendron, A.J., Jr., E.J. Cording, and A.K. Aiyer, “Analytical and Graphical Methods for the Analysis of Slopes in Rock Masses,” Technical Report GL-80-2, prepared for U.S. Army Engineer Waterways Experiment Station, Vicksburg, Mississippi, March 1980.

Ladanyi, B., and G. Archambault, “Shear Strength and Deformability of Filled Indented Joints,” International Symposium on the Geotechnics of Structurally Complex Formations, vol I, pp. 317-326, Capri, 1977.

Londe, P., Rock Mechanics and Dam Foundation Design, International Commission on Large Dams, Paris, 1973.

Mills-Bria, B.L., L.K. Nuss, D. Harris, and D.R.H. O’Connell, “State-of-Practice for Non-Linear Analysis at the Bureau of Reclamation,” Bureau of Reclamation, Technical Service Center, Denver, Colorado, January 2006.

Powell, C.N., P.T. Shaffner, and J. Wright, “Exploration and Geotechnical Characterization for Evaluating the Stability of Hungry Horse Dam,” Proceedings, USSD Conference, Portland, Oregon, April 2008.

Rengers, N., “Influence of Surface Roughness on the Friction Properties of Rock Planes,” Proceedings, 2nd ISRM Congress, Belgrade, vol VI, pp. 229-234, 1970.

Scott, G.A. and B.L. Mills-Bria, “Nonlinear, 3-D, Dynamic, Coupled Dam-Foundation Analyses for Estimating Risks at Hungry Horse Dam,” Proceedings, USSD Conference, Portland, Oregon, April 2008.

Scott, G.A., “The Practical Application of Risk Analysis to Dam Safety,” Keynote Paper, GeoRisk, ASCE, pp. 129-168, 2011.

Scott, G.A., “Guidelines, Foundation and Geotechnical Studies for Existing Concrete Dams,” Bureau of Reclamation, Technical Service Center, Denver, Colorado, September 1999.